Infrared Optical Dating of Organic-rich Sediments

by

Jinsheng Hu

B.Sc., Peking University, 1985

M.Sc., Institute of High Energy Physics, Academia Sinica, 1988

A THESIS SUBMITTED IN PARTIAL FULFILLMENT
OF THE REQUIREMENTS FOR THE DEGREE OF
MASTER OF SCIENCE
in the Department
of
Physics

SIMON FRASER UNIVERSITY
August 1994

APPROVAL

Name: Jinsheng Hu

Degree: Master of Science

Title of thesis: Infrared Optical Dating of Organic-rich Sediments

Examining Committee: Dr. E.D. Crozier
Chair

Dr. D. J. Huntley
Senior Supervisor

Dr. R. F. Fründt

Dr. G. Kirczenow

Dr. K. E. Rieckhoff
Examiner

Date Approved: Aug 3/94

PARTIAL COPYRIGHT LICENSE

I hereby grant to Simon Fraser University the right to lend my thesis, project or extended essay (the title of which is shown below) to users of the Simon Fraser University Library, and to make partial or single copies only for such users or in response to a request from the library of any other university, or other educational institution, on its own behalf or for one of its users. I further agree that permission for multiple copying of this work for scholarly purposes may be granted by me or the Dean of Graduate Studies. It is understood that copying or publication of this work for financial gain shall not be allowed without my written permission.

Title of Thesis/Project/Extended Essay

Infrared optical dating of organic-rich sediments.

Author: _____
(signature)

Mr. Jinsheng Hu
(name)

Aug 11/94
(date)

Abstract

The dating of sediments using infrared stimulated luminescence has drawn very much attention in recent years, especially because of the simplicity of the apparatus by which such luminescence can be measured. On the other hand, the applicability of the technique for age determination has not yet been demonstrated satisfactorily so far. This work is an attempt to investigate whether or not the infrared optical dating technique could produce correct ages for organic-rich sediments. Five of the seven samples studied yield satisfactory ages ranging from 0 up to about 100 ka. Two of the samples are of well-established ages while another three yield ages which are consistent with other evidence. It was also found that inhomogeneities in this type of sediment can be large enough to destroy the validity of the optical age. For the oldest sample studied (the age of which is between 0.78 and 1.06 Ma), the optical ages was found to be 706 ± 98 ka.

Additionally, a possible lower limit of 290 ± 30 ka was obtained for the age of a sand sample collected from the Diring Yuriakh stone tool site.

Acknowledgements

I wish to express my deepest gratitude and appreciation to my senior supervisor, Professor D.J. Huntley, for his intellectual guidance and continuing support throughout the research. I also take the pleasure to thank the other members of my supervisory committee: Professor R.F. Frindt and Professor G. Kirczenow, for their expertise and guidance. I wish to thank the internal examiner, Professor K.E. Rieckhoff for his time and valuable comments.

Mr. O.B. Lian should be specially thanked for generously supplying the geological details of all the organic-rich samples collected for this work. The kind assistance of Mr. G. Morariu in sample preparation is gratefully acknowledged.

The financial assistance from my supervisor Dr. D.J. Huntley through his grant from the Natural Sciences and Engineering Research Council of Canada, and the teaching assistantships from the Physics Department are also gratefully acknowledged.

Finally, I thank all the secretarial and technical staff of the Physics Department and the personnel in the SFU machine shop and electronic shop for their assistance during the years.

Contents

List of Tables

List of Figures

Chapter 1

Introduction

The application of photoluminescence (or optically stimulated luminescence) for age determination was first introduced by Huntley *et al.* (1985). Subsequent work by Hütt *et al.* (1988) showed that infrared light of about 1.4 eV could be used to stimulate photoluminescence from old potassium feldspar samples. Because of the simplicity of this measurement, more and more attention has been paid to this technique in recent years. But up till now, most of the reported work on optical dating using infrared excitation has been on studies of the physical processes and possible explanations of such a phenomenon. The applicability of the technique for age determination has not yet been demonstrated satisfactorily. This work is an attempt to investigate whether or not the technique could produce correct ages for organic-rich sediments with ages between 0 and about 800 thousand years.

1.1 Dating making use of photoluminescence

In optical dating, *photoluminescence* or *optically stimulated luminescence* usually refers to the emission of light from a crystalline material as a result of stimulation by light with lower photon energy than that of the emitted light. The crystalline material must have been exposed to ionizing radiation in order to observe the photoluminescence. This phenomenon can be explained using the energy band theory of solids. A simple band model for a crystalline material is schematically shown in figure 1.1,

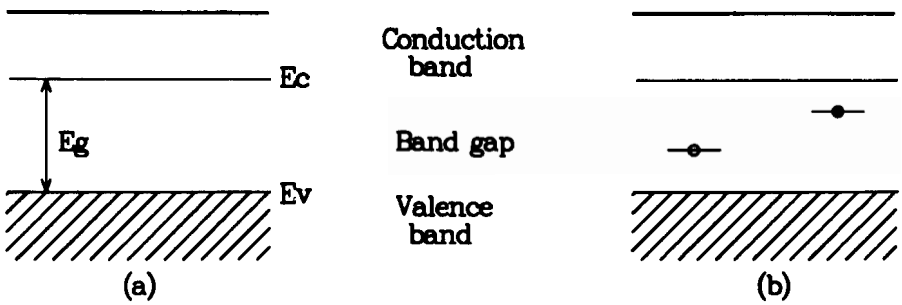

Figure 1.1: A simple band model of solids. (a) ideal crystal; (b) crystal with defect energy levels.

where E_c is the lowest energy of the conduction band, E_v is the highest energy of the valence band, and E_g is the band gap. For ideal materials, as shown in figure 1.1(a), optical absorption only takes place for photon energy greater than band gap E_g. However, if there are structural defects or impurities in the crystal lattice, the periodicity of the crystalline structure is interrupted, and it becomes possible for electrons to possess energies which are not allowed in a perfect crystal (figure 1.1(b)). The new defect energy levels are localized, and may be discrete or distributed. These defects are often referred to as *traps* or *recombination centres* depending on the relative probability of trapping and recombination at a given temperature. The energy required to release an electron from a trap is less than that required to free an electron from the valence band. The same argument is also applicable to holes. The mean thermal lifetime, τ, for trapped charge carriers is given by (Aitken 1985, p.50):

$$\tau = s^{-1} \exp(E/kT) \tag{1.1}$$

where s ($\sec^{-1}$) is the frequency factor and E is the trap depth, *i.e.* the energy difference between E_c for electrons (E_v for holes) and a defect energy level; k is Boltzmann's constant, and T is the absolute temperature.

The absorption of ionizing radiation of energy $E > E_g$ results in the ionization of valence electrons, producing free electrons in the conduction band and free holes in the valence band. The free electrons and free holes may either recombine with each other, or become trapped at defects, or recombine at a defect site. It can be shown that the direct recombination of free electrons and free holes is a less likely process

than the recombination at a defect site (Mckeever 1985, p.33). The number of trapped electrons or holes is thus a measure of the amount radiation energy or radiation dose received by a crystal.

Photons can stimulate some of the previously-trapped electrons or holes back into the conduction or valence band, respectively. Some of these freed electrons or holes may then recombine at respective recombination centres and emit luminescence. Traps that can be emptied by sufficient light exposure are usually referred to as *light-sensitive* traps. The intensity of the photoluminescence is a measure of the total number of trapped electrons and holes which are sensitive to light, and is thus a measure of the total amount of radiation dose received by a crystal since the time when all the light-sensitive traps were last emptied.

The age of a sediment, which is defined here as the time elapsed since the last time when all the light-sensitive traps were emptied, *i.e.* since the time when the sediment was last exposed to sufficient sunlight, can be determined from the absorbed radiation dose and the dose rate:

$$\text{age} = \frac{\text{absorbed radiation dose}}{\text{dose rate}} \tag{1.2}$$

The natural environmental dose experienced by sediments mainly comes from α, β and γ rays emitted by radioactive substances both in the sediments to be analyzed and in the surroundings, chiefly isotopes of uranium, thorium and potassium. If, as is often the case, the decay of these isotopes reached secular equilibrium millions of year ago, the natural dose rate from these radioactive materials is effectively constant. Therefore, equation(1.2) is valid for sediments if the following conditions are satisfied: 1) the rate of thermal release of trapped electrons and holes during the radiation time was negligible; 2) all light-sensitive traps were emptied at time of deposition.

If the above conditions are satisfied, optical dating should be of use to date sediments of ages from 0 to probably 1 million years depending on the dose rate, the upper limit occurring due to the traps becoming full.

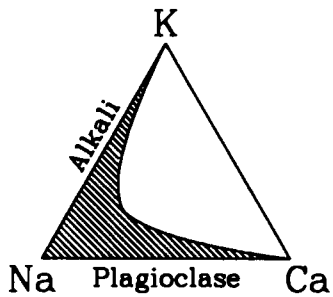

Figure 1.2: feldspars ternary diagram. The shaded area indicates the range of observed compositions.

1.2 Feldspars

Since infrared optical dating is performed only on feldspars, the properties of feldspars that are related to dating are briefly discussed here. The majority of feldspars are composed of varying proportions of *orthoclase* ($KAlSi_3O_8$), *albite* ($NaAlSi_3O_8$), and *anorthite* ($CaAl_2Si_2O_3$), which are also referred to as potassium, sodium and calcium feldspars, respectively. Members of the series between orthoclase and albite are called *alkali feldspars*, and those between albite and anorthite are called *plagioclase* (figure 1.2). Most natural feldspars are not homogeneous but contain separate potassium rich and sodium rich phases. In addition, for each chemical composition, there are two or more crystalline phases, for example, both microcline and sanidine are potassium feldspar. The density of plagioclase feldspar ranges from 2.62 to 2.76 g/cm^3, and that for alkali feldspars from 2.56 to 2.63 g/cm^3 (Deer *et al.* 1966).

Although feldspars have been used for thermoluminescence and photoluminescence dating for quite some time, there is still little information about the electronic structure of feldspars, such as the band gap (approximately 5 eV as is used by Spooner 1994, p.115), trap types, trap depths, *etc.*. Some reported values for trap parameters relevant to dating applications are listed in table 1.1. It should be noticed that the thermal lifetime of electrons in traps with a depth 1.4 eV is not sufficient for thermal stability on a geological time scale, yet it was found (Hütt *et al.* 1988) that the photoluminescence induced by 1.4 eV infrared light is associated with quite stable traps and may be used for dating. This reason for this is still not fully understood.

Table 1.1: Trap depths and lifetimes of K-feldspars at 15 °C*

Trap depth (eV)	0.76	1.10	1.40	1.62	1.60(?)
Frequency factor (sec^{-1})	6×10^9	1.3×10^{13}	2.8×10^{13}	4.1×10^{13}	1×10^{13}
Half life (years)	0.16×10^{-3}	43×10^{-3}	3.6×10^3	3.9×10^6	1×10^9

*from Aitken 1985, p.272

Investigations have also been made on the emission spectra of feldspars (see section 1.3); as yet identities of all the luminescence centres have not been determined. An emission band at ~2.2 eV (570 nm) is attributed to Mn^{2+} luminescence centres. All the other emission bands, especially the 3.1 eV (400 nm) band for potassium feldspars, which is of particular interest in optical dating, are still not definitely associated with any defect (Marfunin 1979). It has been shown that for alkali feldspars, the 3.1 eV emission band dominates and the stimulated luminescence intensity is greatest for samples with the highest potassium contents; for plagioclase feldspars, the 2.2 eV emission band dominates and that the luminescence intensity is greatest for samples with the highest sodium contents (Prescott and Fox 1993, Huntley *et al.* 1988).

1.3 Literature review

The possibility of dating sediments with photoluminescence was first proposed by Huntley *et al.* in 1985. Green light (2.4 eV, 514.5 nm) from an argon laser was used to stimulate photoluminescence from both quartz and feldspar samples in their experiments. Subsequent work by Hütt *et al.* (1988) showed that infrared light with photon energies of 1.2—1.5 eV (1000—800 nm) can be used for stimulating photoluminescence from potassium feldspars. The infrared stimulated photoluminescence was believed to result from quite stable traps and thus be useful for dating. Several papers have been published since infrared optical dating was proposed, however, most of the reported works were studies of the phenomenon and possible physical processes of infrared stimulation, and little work was done on the application of such a technique to date natural sediments.

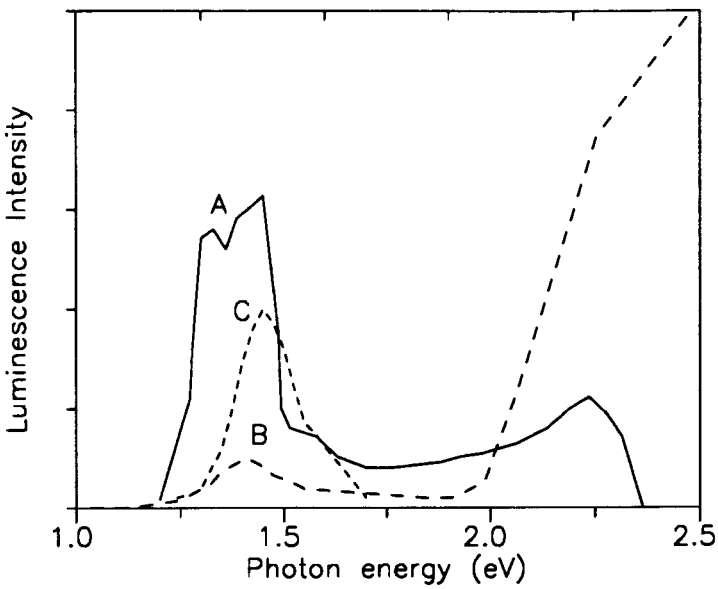

Figure 1.3: Excitation spectra of feldspars. A. after Hütt and Jaek 1989; B. from Bailiff and Poolton 1991; C. Bailiff 1993. Curves were scaled vertically for clarity.

1. Excitation spectra

The dependence of luminescence intensity on stimulation photon energy was first investigated by Hütt *et al.* (1988) using a Xe lamp as a light source. Luminescence at ~3.1 eV (400 nm) was observed during stimulation with 0.8—2.3 eV photons (1500—550 nm). A broad double-peak resonance band was observed in region of the near infrared at 1.2—1.5 eV, wavelength 1000—800 nm. The results were confirmed later by similar measurements using a pulsed excimer dye laser (Hütt and Jaek 1989). The excitation spectrum from the latter is shown in figure 1.3.

A similar resonance band was also found by later studies for an orthoclase feldspar sample with a tunable laser (Bailiff 1993, also see figure 1.3), but only a single-peak band was observed.

Another type of experiment was to bleach museum feldspar samples with photons of different photon energies and to observe the resulting luminescence stimulated by 1.31 eV (940 nm) photons (Bailiff and Poolton 1991). The resonance band was also found to consist of a single peak for the feldspar samples studied.

The decrease of luminescence intensity for stimulation photon energies greater

than about 2.2 eV (Hütt *et al.* 1988, Hütt and Jaek 1989, see figure 1.3) was not observed in other studies (Bailiff and Poolton 1991, Ditlefsen and Huntley 1994). It was speculated that the increase instead of decrease at the higher energy end was due to the direct optical excitation of the luminescence centres (Bailiff and Poolton 1991).

Stimulated luminescence from feldspar extracts of a sediment was observed using each of the six wavelengths from a krypton laser (1.55+1.65 eV (799+753 nm), 1.92 eV (647.1 nm), 2.18 eV (568.2 nm), 2.34 eV (530.9 nm), 2.65 eV (468 nm), and 3.00 eV (413 nm)), and a similar equivalent dose was obtained for each of the wavelengths used (Godfrey-Smith *et al.* 1988). This indicates that the equivalent dose of a sediment measured with photoluminescence does not depend on the photon energy of the stimulation light.

2. Emission spectra

Stimulation of feldspars with laser photons at 1.96 eV (633 nm) from a He-Ne laser (Jungner and Huntley 1991), 2.41 eV (514 nm), or infrared diodes with peak emission at 1.4 eV (880 nm) (Huntley *et al.* 1991) gives rise to emission spectra with peaks at 3.8 eV (330 nm), 3.1 eV (400 nm) and 2.2 eV (570 nm). Particularly strong 3.1 eV (400 nm) bands for potassium feldspars and 2.2 eV (570 nm) bands for plagioclase feldspar were observed. The emission spectra stimulated by 1.31 eV infrared diode arrays for various kind of feldspars gave similar results (Bailiff and Poolton 1991).

3. Thermal stability

The thermal stability of infrared stimulated luminescence was studied by measuring the luminescence signal at a fixed temperature after rapidly heating sedimentary feldspar samples (loess) to successively higher temperatures (Li and Wintle 1992). It was observed that there was no loss in luminescence signal until a temperature of 200 ℃ was attained. Also, a short term unstable luminescence signal[1] for the laboratory irradiated samples was observed and preheating of samples was suggested to be necessary to remove this component prior to dating measurements.

Work by Spooner (1993, p.162, p.184) concluded that there was no physical basis for the existence of an age limit for coarse grain feldspars other than dose saturation,

[1]The unstable luminescence signal refers to the luminescence signal that disappears after the sample has been stored for a period of time.

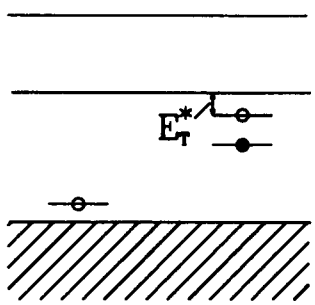

Figure 1.4: Thermo-optical model proposed by Hütt *et al.* 1989. it was suggested that infrared light excites electrons to traps of intermediate depths where additional energy, E_T^* (thermal activation) causes a transition to the conduction band.

and there appeared to be an age limit of 100 ka for fine grain feldspars.

4. Thermo-optical model

The phenomenon that infrared light can stimulate luminescence from thermally stable traps is still a mystery. In the model proposed by Hütt *et al.* (1989), it was suggested that infrared light excites electrons to traps of intermediate depths where additional energy (thermal activation) causes a transition to the conduction band, as illustrated in figure 1.4. Hütt *et al.* suggest that the last process is expected to be exponentially dependent on temperature as:

$$I = I_0 \exp(E_T^*/kT) \tag{1.3}$$

with I and I_0 being the photoluminescence intensity at a temperature T and at room temperature (T_0) respectively, and E_T^* being the thermal activation energy. Equation (1.3) was quoted from Hütt *et al.* (1989) and it seems the equation cannot be correct; I_0 is not returned when $T = T_0$, and it predicts that I *decreases* with temperature. The correct equation might be as the following:

$$I = I_0 \exp\left(\frac{E_T^*}{kT_0} - \frac{E_T^*}{kT}\right) \tag{1.4}$$

Measurements based on this model yielded a value for E_T^* of 0.2 ± 0.1 eV (Hütt *et al.* 1989). Later work by Duller and Wintle (1991) gives a value of 0.15 ± 0.02 eV for a natural potassium feldspar sample extracted from a dune sand; Bailiff and

Poolton (1991) give values of about $0.10 \pm 0.02\,\mathrm{eV}$ for a museum feldspar specimen. The extensive work of Spooner (1993), on the other hand, showed that E_T^* varies from $0.087\,\mathrm{eV}$ to $0.278\,\mathrm{eV}$ for various feldspar samples and that there might be a dependence of E_T^* on the major composition of the feldspar being studied.

Unfortunately, this model is still full of difficulties and appears to be too simple to account for all the experimental results. Additionally, there still isn't a full mathematical treatment for such two step transitions and for the thermal life-time of trapped electrons in such a case. It is also expected according to the model that the integrated photon emission should be the same regardless at what temperature such luminescence was measured, and yet it was observed that such photon emission increases with the temperature of measurement [2](Duller and Wintle 1991, Short 1993). This is still unexplained and casts doubt on the validity of the E_T^*'s obtained by the analyses.

5. Dating

The first infrared optical dating results were reported by Hütt *et al.* (1988) on several eolian, alluvial and marine samples, the ages of which were between 5 and 50 ka. The dating results appeared to agree with the geological estimates, but since no details of the samples, the basis of their known ages or the dosimetry were given, it is difficult to evaluate the results.

Aitken and Xie (1992) reported the optical dates of some alluvial and colluvium sediment samples from England with ages from 1 to 5 ka which showed good agreement with the dates from other methods. The equivalent doses were obtained using a subtraction technique. The samples were preheated for 1 hour at 160℃, 3 days at 100℃, and >1 day at 20℃, and no reason was given for such a treatment. The uncertainties for the dates varied from sample to sample and ranged from 11% to 37%.

Hütt and Jungner (1992) reported dates for three samples from the Yukki area near Leningrad. It was found that the ages from optical dating were far too high for two of the samples. In addition, some buried podsol and overlying sands were also studied

[2]It was also found that at 77 K, emission of luminescence was reduced to almost negligible (Bailiff and Poolton 1991).

and it appeared that optical dates were generally younger than thermoluminescence dates (Hütt *et al.* 1993). It should be noted that samples were not preheated in this work, and this is expected to lead to the ages being too young.

Optical dates for young dune sediments, which were taken from Buctouche Spit, New Brunswick, indicated that the method may be used for dating samples with ages between 0 and 1000 a (Ollerhead *et al.* 1994). The additive dose method was used to determine the equivalent doses in this work. The samples were preheated for 5 days at 120°C, 140°C and 160°C or at 140°C only. The preheat temperature was chosen because other samples at the S.F.U. laboratory yielded equivalent doses consistent with their known ages, and because of a temperature independence of equivalent dose values in this range. The ages obtained were consistent with the historical evidence coupled with an assumed sediment aggradation rate.

Before general reliance can be placed on optical dating, it is necessary to show that correct ages can be obtained on known-age samples. The requirements for this are (Ollerhead *et al.* 1994): 1) properly documented samples, with ages which are well established and that can be associated with the last exposure to sunlight, and 2) documented procedures that can be justified on the basis of our understanding of the physics. It is clear that more tests are still needed to attain such a goal.

1.4 Papers on optical dating using infrared excitation

Papers that are related to optical dating of feldspars using infrared excitation are briefly summarized in the following.

Hütt *et al.* 1988 — excitation spectra; proposed using infrared as a stimulation source; thermo-optical model; some preliminary dating results.

Hütt and Jaek 1989 — Modified thermal-optical model; thermal activation energy E_T^* measured to be 0.2 ± 0.1 eV .

Bailiff and Poolton 1991 — excitation spectra by photons (UV—infrared) and emission spectra for various museum feldspar samples; thermal activation energy

E_T^* measured to be about 0.10 ± 0.02 eV.

Duller and Wintle 1991 — Integrated luminescence increases with temperature. Thermal activation energy E_T^* was measured to be 0.15 ± 0.02 eV for a natural K-feldspar sample extracted from a dune sand.

Li and Wintle 1992 — Thermal stability of infrared stimulated luminescence of loess samples; no loss of photoluminescence signal until a temperature of at least 200 °C.

Aitken and Xie 1992 — Satisfactory dates of alluvium and colluvium samples with known ages between 1 and 5 ka.

Hütt and Jungner 1992 — Dates for three samples from the Yukki area near Leningrad.

Huntley *et al.* 1993 — Dating of feldspar inclusions within quartz. This method gave acceptable ages in the range 0—400 ka for quartz extracted from seven dunes of the stranded beach-dune sequence in south-east South Australia.

Short 1993 — Increase in luminescence emission with sample temperature. The date obtained for a geological sample using additive dose method was in agreement with other dating estimates.

Spooner 1993 — Luminescence properties of various kind of feldspars relevant to dating, such as radiation dose-sensitivities, emission spectra, bleaching with infrared, *etc.*; anomalous fading; long-term trapping stability of the IRSL (infrared stimulated luminescence) source traps.

Hütt *et al.* 1993 — Dates of some buried podsol and overlying sand samples.

Bailiff 1993 — Excitation spectrum for photon energies between 1.2—1.7 eV; a single band was found with a peak at 1.4 eV.

Ollerhead *et al.* 1994 — Dates for a sequence of young dune sediments with ages less than 1 ka; the dates are consistent with independent evidence.

1.5 Overview of later chapters

The work presented in this thesis is an investigation of the possibility of applying the infrared optical dating method to determine the ages of organic-rich sediments. The instruments and details of the selected samples are described in chapters 2 and 3, respectively. In the subsequent chapters the determination of equivalent doses and the evaluation of dose rates will be discussed. A discussion of the ages obtained is given in chapter 6.

The preparation procedures for both the fine-grain and coarse-grain samples are listed in appendix A. The results for the sample collected from the Diring Yuriakh site in Russia, where a Paleolithic stone tool assemblage was found, are discussed in appendix B.

Chapter 2

Instrumentation

Optical dating instruments consist of two main components: 1) a light source which illuminates a sample, and 2) a photon detection system which measures the recombination luminescence. A computer controlled instrument, which is capable of measuring up to 50 samples automatically, was used for this work. Infrared diodes were used for the light source to stimulate luminescence from feldspar samples. Photoluminescence was measured with a photomultiplier tube. In this work, the photon energy of the luminescence is larger than that of the photons of incident light.

2.1 Automated 50-sample apparatus

An existing apparatus that was designed to use a laser for the light source (Godfrey-Smith, 1991) was used. The apparatus consists of a 60-cm diameter turntable with 50 sample holders placed in the circular openings along its rim. The turntable is rotated by a 1:100 ratio worm gear driven by a 7.5°/step stepping motor. The luminescence chamber is located above the turntable, near its edge. An elevator, driven by a second stepping motor, lifts each sample holder in turn, thus putting its sample into the chamber. Control of the apparatus was done using a General Purpose Interface Bus (IEEE 488), a Data Acquisition System/Controller(DAS/CONT), and a Sample Changer Control Unit (SCCU). A schematic of the whole system is shown in figure 2.1.

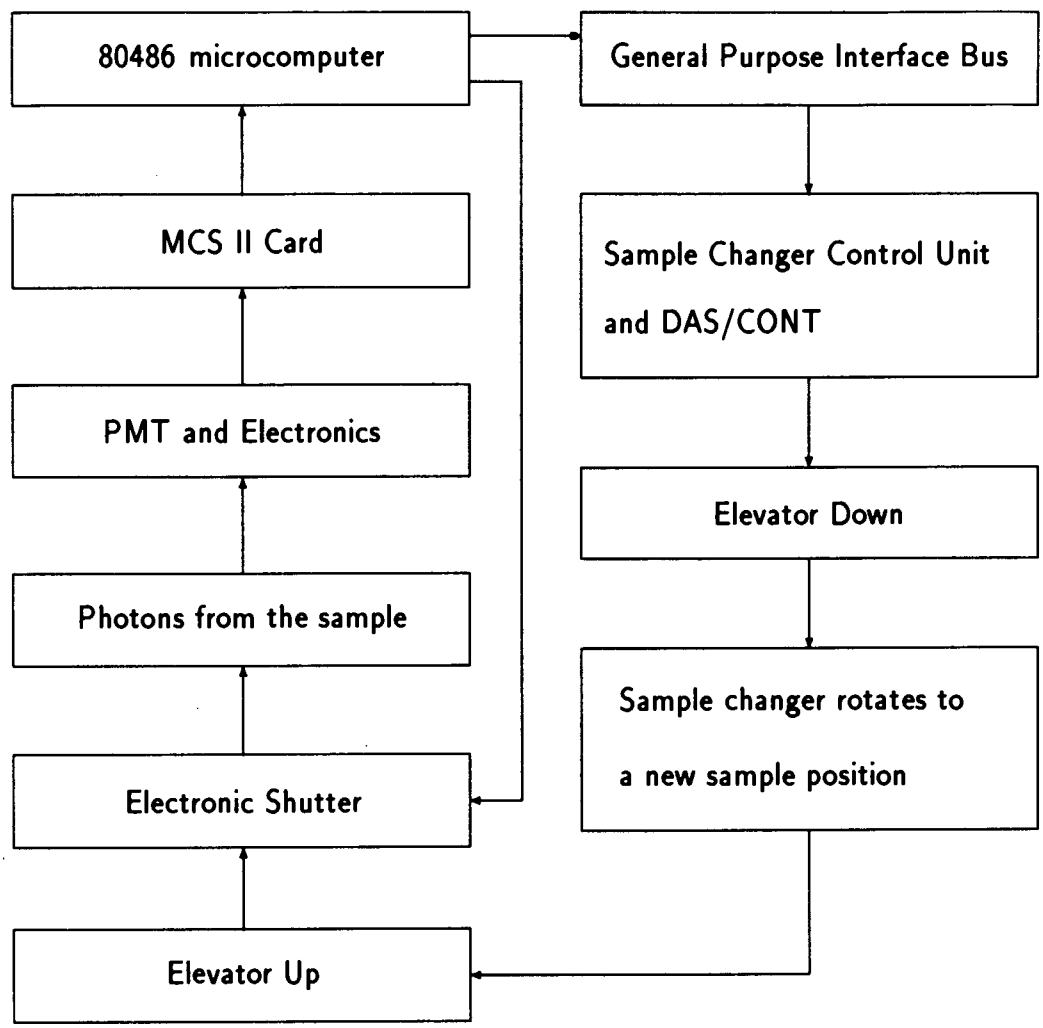

Figure 2.1: Schematic of the automated 50-sample apparatus

The luminescence chamber was adapted for the use of infrared diodes instead of a laser for illuminating a sample. A specially designed diode holder (figure 2.2) with 31 infrared diodes was placed inside the luminescence chamber. The orientations of the diodes were arranged so that all the diodes are pointed to the centre of the sample, as shown in figure 2.3. An electronic shutter was used to start or stop the illumination of the sample.

Stanley[1] infrared diodes (model CN305) were used as the light source. The specifications show the emission band to be 880 ± 50 nm, with a half intensity angle of 18 degrees. The total power of 31 diodes on the sample was measured to be $20\,\mathrm{mW/cm^2}$ when the diode current was set to 60 mA.

One Schott BG39 (2 mm thick) optical filter was used to prevent scattered infrared light from reaching the photomultiplier tube. The transmission curve for BG39 filter is shown in figure 2.4.

An EMI 9635 photomultiplier tube (PMT) was used for photon detection; its quantum efficiency is also shown in figure 2.4. The electronics included a high-voltage power supply to the PMT, a preamplifier and an amplifier-discriminator. Negative logic pulses from the discriminator were fed into a multichannel scaler card[2] (200 MHz, 8192 bytes on board memory) installed in an 80486 microcomputer. The data were immediately placed on the computer hard drive for further analysis.

There are 50 sample holders on the 50-sample apparatus marked from #1 to #50. The reproducibility of the apparatus was tested to make sure that all these 50 sample positions were equivalent, *i.e.*, each sample would produce the same amount of luminescence no matter where it was and when it was measured. This was done by measuring luminescence from 5 sample discs containing grains of a bright K-feldspar at different sample positions and at different times. The procedure was as the following:

1. Turn on the diodes for 30 minutes to have them warmed up.
2. Mount samples on positions #2 to #6 (position #1 was always reserved for testing the devices) and measure the luminescence from each sample for 5 seconds.

[1] Purchased through Deskin Inc., Vancouver

[2] MCS-II, manufactured by Tennelec/Nucleus Inc., 601 Oak Ridge Turnpike, Oak Ridge, Tennessee, USA 37830

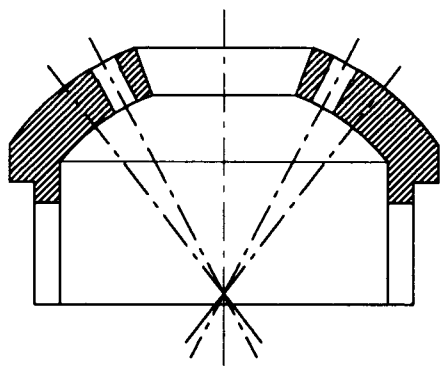

(a) side view

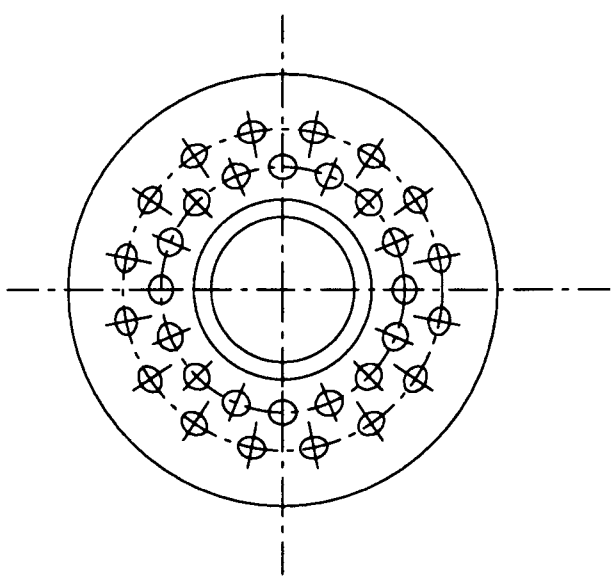

(b) top view

Figure 2.2: Infrared diode holder. One of the diode positions is not used.

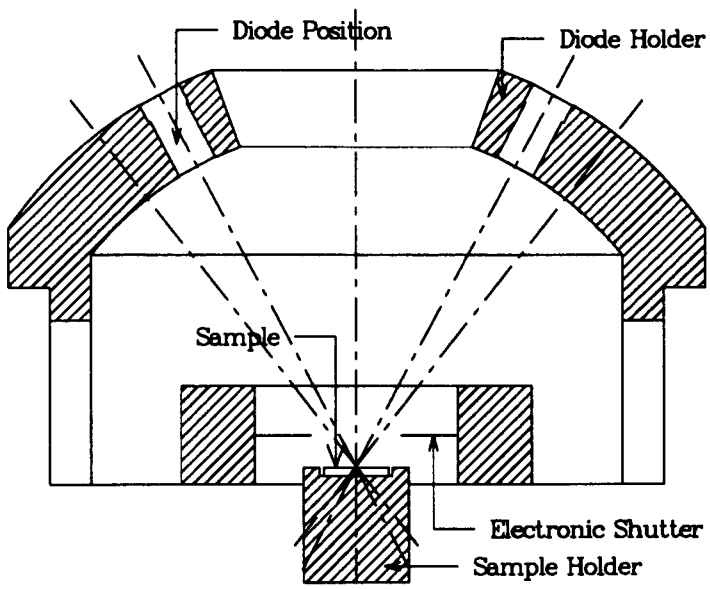

Figure 2.3: Luminescence chamber

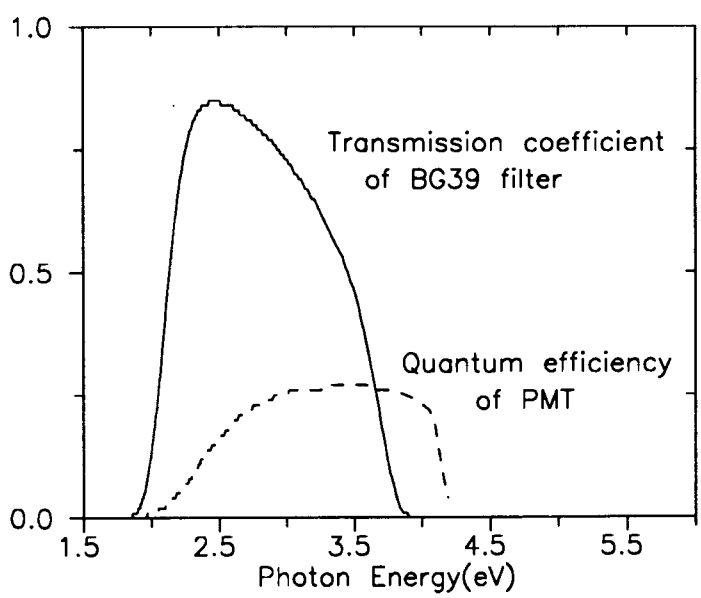

Figure 2.4: Transmission vs. wavelength for the Schott BG39 optical filter and quantum efficiency for the photomultiplier tube

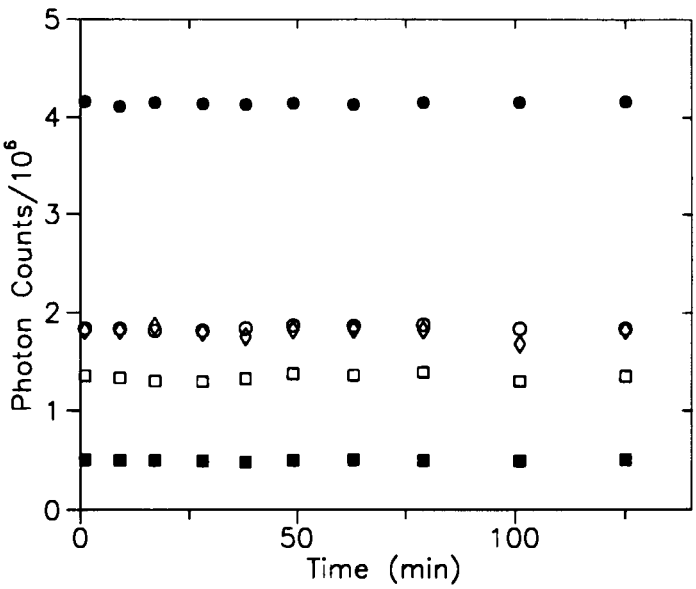

Figure 2.5: Reproducibility of the 50-sample apparatus. Photon counts measured for 5 different samples in different positions of the apparatus. The horizontal axis indicates how long the diodes had been on after the 30 minutes warming period. Each symbol represents one of the five samples.

3. Move samples to positions #7 to #11 and wait for about 10 minutes before measuring the luminescence again.

4. Repeat step 3 to cover all other sample positions(#12 to #50).

The luminescence intensity from these samples decays over time. This decay can be approximately described as an exponential function. The results in figure 2.5 show the measured luminescence intensity for the above samples after correction for decay.

The ratios of the photon counts for each measurement to the mean photon counts for each sample were then calculated to find the standard deviation. The calculated standard deviation for all the data points in figure 2.5 was 0.3%.

2.2 Laboratory radiation sources

Gamma irradiations were carried out using a ^{60}Co gammacell (half life 27 years). Calibration of the γ source was done by Dr. D.J. Huntley and O.B. Lian in July, 1989

using $CaSO_4$: Dy powder, which was given precisely known ^{60}Co γ exposures at the Ionizing Radiation Standards Laboratory at the National Research Council, Ottawa. The dose rate was determined to be 0.90 Gy/min[3] in July 1989 for SiO_2 on aluminum at a standard position in an aluminum holder. The decay factor of the dose rate is 98.9% per month.

Alpha irradiations were done using six ^{241}Am sources (half life 433 years) in a chamber which was evacuated, after placing samples in it, to avoid attenuating the alpha radiation by air. The dose rates for the six sources were 0.381, 0.371, 0.413, 0.383, 0.394, and 0.370 $\mu m^{-2} min^{-1}$, respectively[4]. These dose rates were provided by the Laboratory for Research in Archaeology and the History of Art in Oxford.

[3] 1 Gy=1 J/Kg.

[4] The luminescence due to α irriadiation is proportional to the total track length of all α particles, rather than their energy. The α radiation dose is thus defined in the unit of α particle track length per unit volume.

Chapter 3

Sample Descriptions

A set of peat sediment samples was selected for testing the infrared optical dating method. The locations and site sections of these samples are shown in figure 3.1—3.3. Peat samples were chosen for the following reasons: 1) peat is formed from a slow accumulation of organic and mineral materials in standing water. The mineral materials were likely to have arrived from eolian processes. Therefore, the electron traps used for optical dating were probably emptied at the time of deposition because the minerals were likely to have had sufficient sunlight exposure. 2) The movement of U and Th is governed by the movement of humic and fulvic acids which are strongly bound to clay materials (Van der Wijk *et al.* 1986), thus the mobility of U and Th in organic clayey deposits of sufficient thickness ($\geq\sim$10 cm) is low. Therefore, the dose rate from U and Th is likely to be constant.

The ages of the samples collected at Burns Bog, Lynn Valley, and Sumner, were already known. The ages of the samples from Useless Bay and Muir Point were relatively uncertain but severely constrained. The purpose of the study was first to find out whether or not correct ages can be obtained for known-age peat samples with this optical dating method, and then to determine the ages for the unknown-age samples.

Peat samples selected for this work are described in the following (from the youngest to the oldest):

BBP3 Collected at Burns Bog, British Columbia. This is a modern peat that is

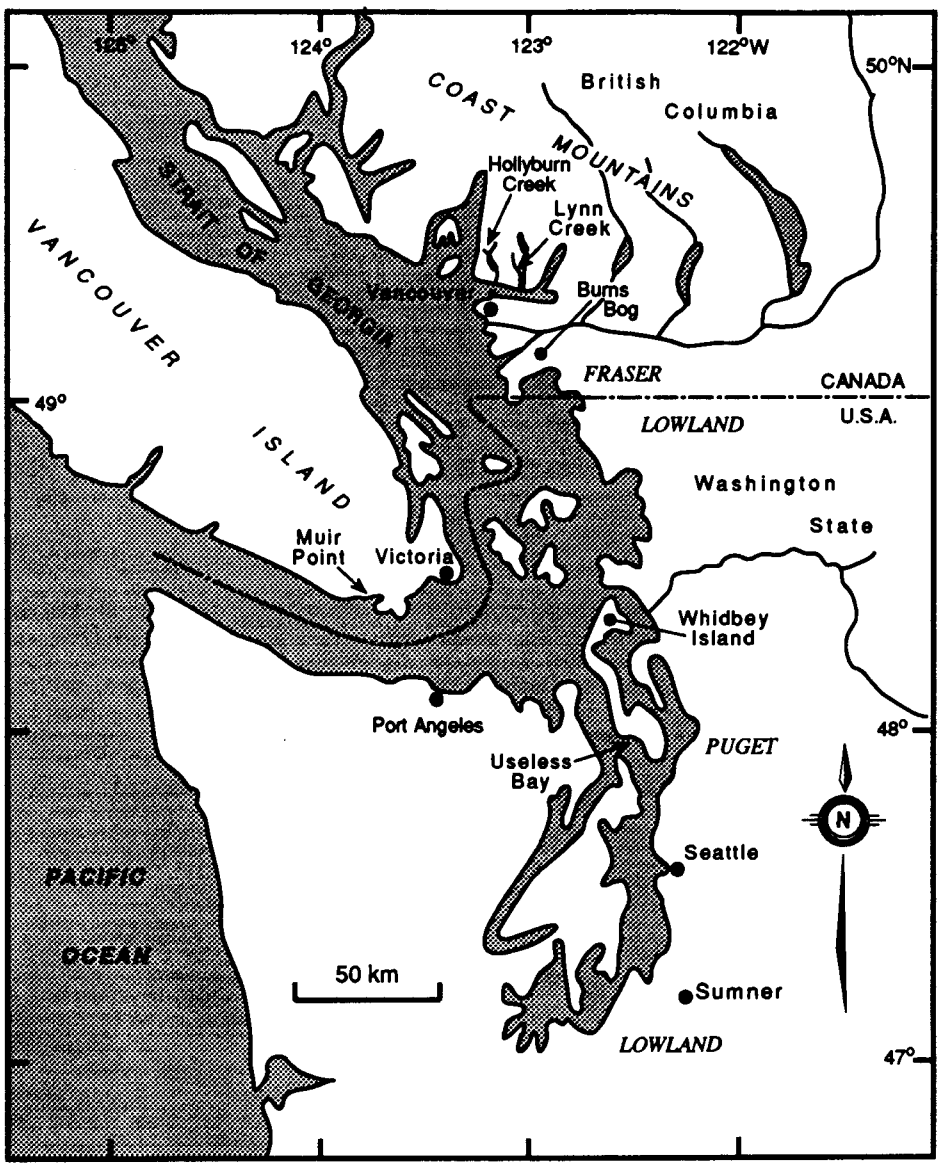

Figure 3.1: Sample Locations (provided by O.B. Lian)

forming on the Fraser Delta. The sample used was collected by Divigalpitya (1982). The sample was located 25 cm below the surface. The upper limit of the age for this sample was estimated to be less than 0.5 ka (Divigalpitiya 1982; Huntley *et al.* 1983). It was selected in order to determine if a modern sample would give a zero age with the infrared optical dating method.

LCP5 Collected in Lynn Valley, North Vancouver, British Columbia. The Cowichan Head Formation(Armstrong and Clague 1977; Ryder and Clague 1989) (see figure 3.2) includes sediments deposited during the Olympia Nonglacial Interval. In Lynn Valley, the Cowichan Head Formation includes about 1 m of compressed peat containing a 1-cm-thick sand bed. Radiocarbon dating has shown that the peat in Lynn Valley was deposited between 47,800±1,100 BP[1] (GSC-290) and 33,100±620 BP (GSC-2797) (Armstrong 1990). Sediment extracted from the peat, just above the sand bed (figure 3.2), has yielded a TL age of 25±4 ka (LCP3) (Divigalpitiya 1982; Huntley *et al.* 1983). A ^{14}C date of 34,900±810 BP (GSC-2873) was also obtained from this position. For this study, peat from the same stratigraphic position as LCP3 was sampled (LCP5).

MPS1 & MPS2 Collected at Muir Point, British Columbia. The Muir Point Formation (figure 3.3) is a major Pleistocene nonglacial lithostratigraphic unit that occurs on southern Vancouver Island (Hicock and Armstrong 1983; Alley and Hicock 1986; Hicock 1990). All radiocarbon ages from the Muir Point sediments are upper limits only. Paleomagnetic studies indicated that the formation was younger that 790 ka BP (Hicock 1990). Based on lithology, stratigraphic position and palynology, these two samples have ages similar to WFP1 and WFP2-6 (Hicock and Armstrong 1983), which are described next.

WFP1 & WFP2-6 Collected at Useless Bay, Whidbey Island, Washington. The Whidbey Formation (figure 3.2) consists generally of silt, sand, gravel and peat deposited in the Puget Lowland during the last (Sangamonian) interglacial (Easterbrook *et al.* 1967; Heusser and Heusser 1981; Blunt *et al.* 1987). Here,

[1]BP: before present (AD 1950). The radiocarbon date is calculated from the ^{14}C to ^{12}C ratio relative to the international standard assuming that the half life of ^{14}C is 5568 years.

the Whidbey Formation includes two organic-rich units, samples of which are named WFP1 and WFP2, surrounded by stratified sand silt and gravel. WFP1 consists of ~2 m of interbedded peat and silt, and WFP2 consists of ~1 m of highly compressed peat. WFP2-6 is a subsample of WFP2. All radiocarbon ages from the Whidbey Formation are limits only (Blunt *et al.* 1987). The only chronological information on the Whidbey formation comes from amino acid studies of wood and shell which suggest an age of 100 ± 20 ka (Easterbrook 1986; Blunt *et al.* 1987).

SSP2-6 Collected at Sumner, Washington. Salmon Springs Drift (figure 3.2) represents the third oldest recognized advance of the Cordilleran ice sheet into the Puget Lowland (Easterbrook, 1992). At the Sumner type section, an ~20-cm-thick peat bed overlies ~1 m of silt, which in turn overlies a 30-cm-thick bed of volcanic ash (Lake Tapps tephra). A fission-track age of 0.84 ± 0.22 Ma had been obtained for the tephra here (on zircon) (Easterbrook *et al.* 1981; Westgate *et al.* 1987). However, the best fission track age estimate is 1.06 ± 0.11 Ma (obtained on glass using the isothermal annealing process) from another exposure about 12 km away (Westgate *et al.* 1987). A paleomagnetic reversal found in the silt layer just below the peats indicates that the lower sediments in this layer are older than the Brunhes-Matuyama boundary (780 ka) (Easterbrook *et al.* 1988). In the earlier survey, a thermoluminescence age of $> 480 \pm 90$ ka was obtained for the peat (Divigalpitiya 1982; Huntley *et al.* 1983). The peat bed was once again sampled for analysis.

Peat samples contain primarily organics and minerals. Among these are feldspars that are desired for infrared optical dating. The purpose of sample preparation is to remove carbonates and organics, to separate required-sized mineral grains (4 to 11 μm), and finally to settle the selected mineral grains onto aluminum discs for handling. The resulting extract usually contained quartz, feldspars and other minerals.

The sample discs were prepared by G. Morariu using the fine-grain sample preparation procedure. The procedure is described in Appendix A.

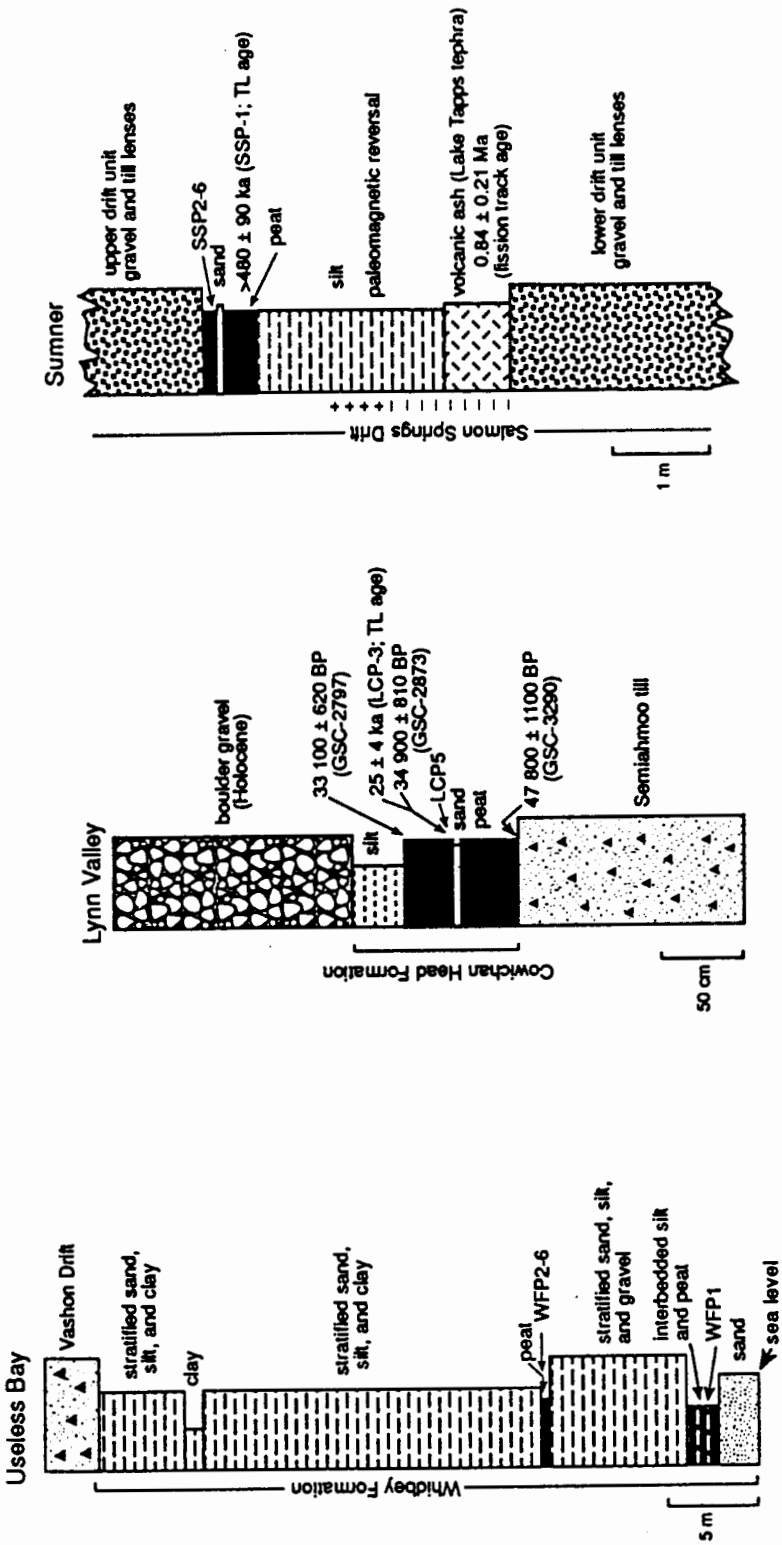

Figure 3.2: Sample site sections (1) (provided by O.B. Lian)

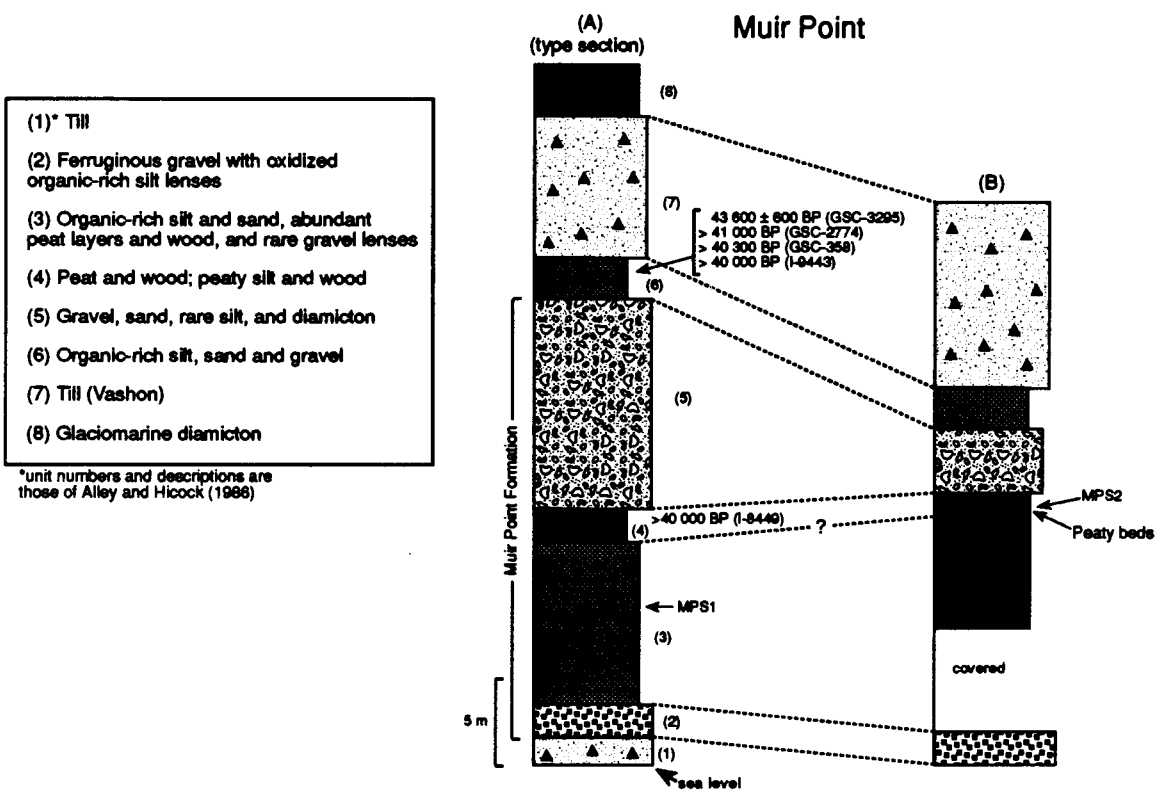

Figure 3.3: Sample site sections (2) (provided by O.B. Lian)

Chapter 4

Equivalent Dose Determinations

Two important factors must be determined in order to find the age of a sediment (which is defined here as the time elapsed since the sediment was last exposed to sunlight): the past radiation dose deposited in the sediment and the radiation dose rate. Dose rate determinations will be discussed in the next chapter.

Because the past dose cannot be measured directly in laboratory, a so-called *equivalent dose*, the laboratory dose which produces the same amount of luminescence as the actual past dose, is determined instead. An additive dose method was used to determine equivalent doses in this work. The obtained equivalent doses will be used to calculate the ages in chapter 6.

4.1 Sample treatment

In order to obtain the equivalent doses, samples were irradiated, bleached, and heated as appropriate to the procedure employed.

1. Irradiations and α effectiveness

Samples are exposed to α, β and γ radiations in the natural environment. The luminescence response to α particles is different from the response to β and γ rays. In the laboratory, both α and γ sources were used to irradiate a sample to determine the α radiation effectiveness (b-value) by comparing the luminescence-dose responses of α and γ irradiated samples. The α effectiveness can be defined as the ratio of the

γ equivalent dose to the α equivalent dose.

2. Bleaching of sediments by sunlight

One of the key assumptions in the optical dating method is that optically stimulated luminescence can be brought to zero through a sufficiently long exposure to the sunlight. The assumption can be confirmed experimentally by observing the luminescence as a function of bleaching time (Godfrey-Smith *et al.* 1988).

In this work, samples were bleached by direct sunlight exposure in order to simulate zero-age samples. The bleaching time was chosen so that after this procedure no optically stimulated luminescence was observed from bleached samples.

3. Heat treatment

In order to obtain a correct age for a sediment, only luminescence which arises from thermally stable traps should be measured. The traps which are not thermally stable on a geological time scale are usually emptied by heating sample discs or planchets in an oven prior to luminescence measurements. Here is an example which shows the effect of heat treatment on the thermal lifetime of trapped electrons. If we assume the frequency factor $s = 10^{13}\,\mathrm{s}^{-1}$ and the thermal trap depth which is related to optical dating is 1.6 eV, then the thermal lifetime of the trapped electrons is about 10,000 ka at room temperature. But if the sample is heated at 140℃ then the thermal lifetime would be reduced to about 38 days. On the other hand, the thermal lifetime of the electrons in shallower traps, say 1.4 eV, will be reduced to about 3 hours. It is therefore clear that such shallow traps are indeed emptied in the process of heat treatment if the above assumptions are valid.

For a sample with low radiation dose and a linear luminescence-dose response curve, the preheating temperature should be chosen in such a range that the ratio $(L_{N+\gamma} - L_{bleached})/(L_N - L_{bleached})$ remains constant regardless of the preheating temperature (Godfrey-Smith 1991); here, $L_{N+\gamma}$ is the luminescence from an irradiated sample, L_N and $L_{bleached}$ are for luminescence from natural and bleached samples respectively. Luminescence from a bleached sample is subtracted from $L_{N+\gamma}$ and L_N to exclude the thermally-induced signal that resulted from thermal transfer of charges into light-sensitive traps.

4.2 Additive dose method

The methods of the equivalent dose determination are based on the following ideas: 1) The exposure to sunlight releases all the trapped electrons which have accumulated in the light-sensitive traps of a sediment. 2) The measured luminescence of these sediments increases with previous radiation dose. The relationship between them can be described by an empirical function, usually a linear or a quadratic function for low doses, and a saturating exponential function for high doses. This empirical curve is usually constructed in the laboratory by applying various amount of radiation doses to a set of identical samples and measuring the resulting luminescence from each sample. Two methods are commonly used to determine equivalent doses, one is the additive dose method, the other is the regeneration method. The latter is discussed in appendix B.

In the additive dose method, various amount of laboratory radiation doses are applied to a number of identical natural samples to construct a luminescence-dose response curve, which is also called a *growth curve.* In order to simulate zero-age samples, some similar samples (N and N+γ) are exposed to sunlight for a certain amount of time, usually a couple of hours, until they will not yield any luminescence when illuminated. The equivalent dose D_e can be obtained by extrapolating the fitted curves of irradiated (N+γ) and bleached (N+γ+sun) data. This is illustrated in figure 4.1.

4.3 Equivalent doses

The additive dose method was used to determine the equivalent doses of all the peaty sediments selected for this work. Bleaching of samples was performed by direct outdoor sunlight exposure for 2 to 3 hours. After irradiation and bleaching, all samples were preheated at 140 ℃ for a week to empty thermally unstable traps (this will be discussed in section 4.4).

Luminescence was measured from natural (N), γ and α irradiated (N+γ, N+α),

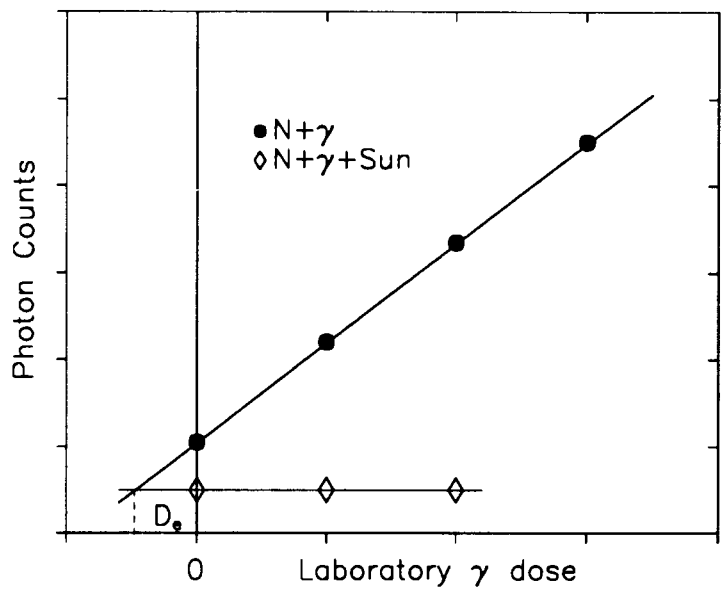

Figure 4.1: Additive dose method. The equivalent dose, D_e, is determined by extrapolating the fitted curves to the (N+γ) and (N+γ+sun) data and finding the intercept.

and bleached (N+sun, N+γ+sun, N+α+sun) sample discs using the automated 50-sample apparatus. The amount of data was then reduced by summing the luminescence data in 50 channel increments (0.1 s per channel, but 0.2 s for MPS1 and MPS2) consecutively, which corresponds to total photon counts for each consecutive 5 s or 10 s intervals along the decay curves.

The growth curve (N+γ) and the bleach curve (N+γ+sun) were obtained by performing a linear or saturating exponential fit to the N+γ data, and a linear or constant fit to the N+γ+sun data, for each 5 s or 10 s interval. The above two curves were then extrapolated to find an intersection, which gives the equivalent dose for each particular interval. The measured luminescence curves and fitting results are shown in figures 4.2 to 4.8. Each luminescence decay curve shown in the figures is the average of measured curves for two different sample discs. The additive dose data in the figures are the photon counts for the first 5 s or 10 s interval of measured luminescence decay curves. The equivalent doses calculated for the different time intervals are shown in figure 4.9. The fitting (maximum likelihood method) and equivalent dose calculation were done using a computer program written by D.J. Huntley. The weighting was

Table 4.1: Equivalent doses & b-values

Sample	γ Equivalent Dose (Gy)	α Equivalent Dose (μm^{-2})	α Effectiveness (b-value) (Gy μm^2)
BBP3	0 ± 1	—	—
LCP5	19 ± 1	22 ± 1	0.86 ± 0.07
MPS1	218 ± 13	190 ± 19	1.15 ± 0.13
MPS2	194 ± 17	173 ± 8	1.12 ± 0.11
WFP1	164 ± 8	203 ± 20	0.81 ± 0.09
WFP2-6	56 ± 5	64 ± 7	0.88 ± 0.12
SSP2-6	246 ± 30	296 ± 65	0.83 ± 0.21

done by inverse variance, appropriate to a constant fractional error that was determined by the fit. The equivalent doses for α irradiations were determined by similar procedures.

An overall equivalent dose for a sample was determined by averaging the equivalent doses for all time intervals. The equivalent doses for all peaty sediments are summarized in table 4.1. The α effectiveness (b-value) was taken to be the ratio of the average γ equivalent dose to the average α equivalent dose. The uncertainties listed in the table are one standard deviation.

4.4 Discussion

The correctness of the equivalent doses obtained above may still be affected by things like anomalous fading, thermal fading, and the depletion of traps due to the initial short exposure for normalization (this was done to the correct for the disc to disc variabilities), *etc.*. Some precautions were taken in the measurement procedures to avoid such problems.

1. Anomalous fading

Fading refers to the loss of luminescence observable with time. Two types of fading have been identified, anomalous fading (usually for laboratory irradiated samples) and thermal fading (due to limited thermal life time of trapped charge carriers), the latter

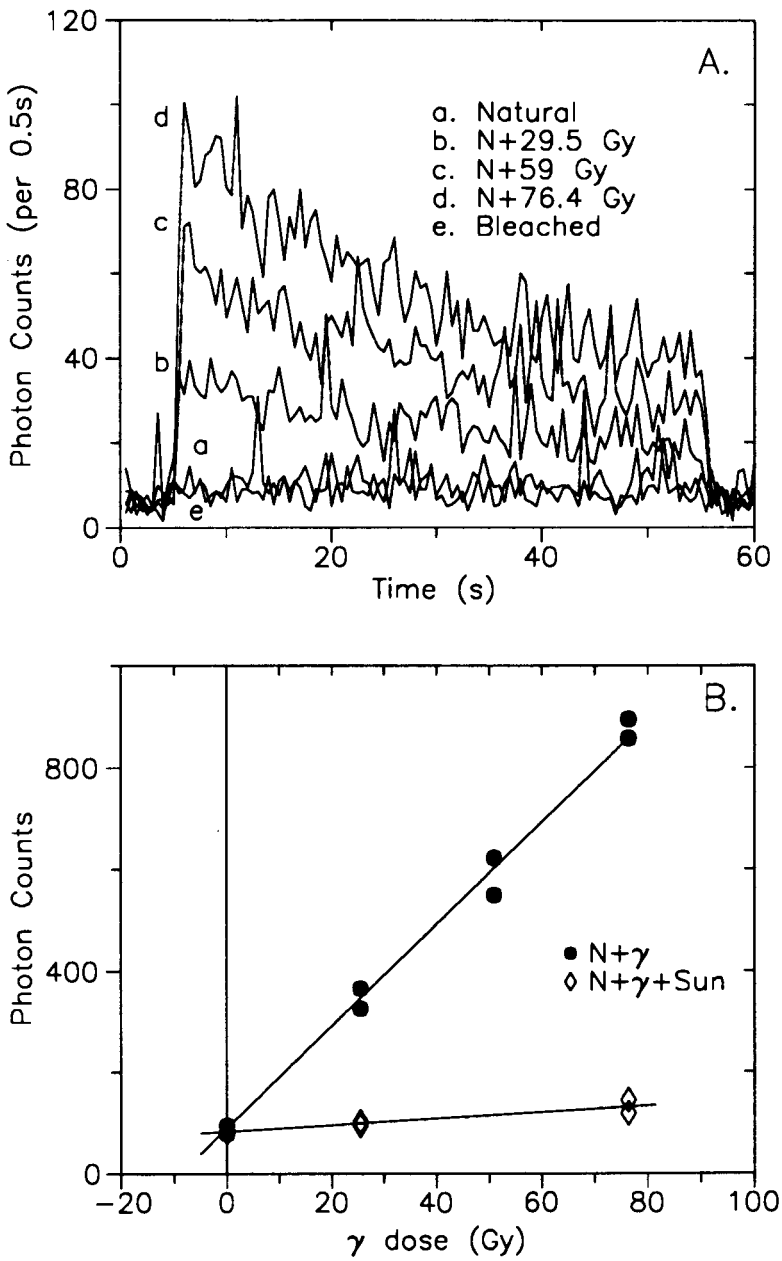

Figure 4.2: Data for BBP3. A. Luminescence decay curves. B. Additive dose data for the first 5 s time interval. Shown is a linear fit to the N+γ data, and and a linear fit to the data for the bleached samples.

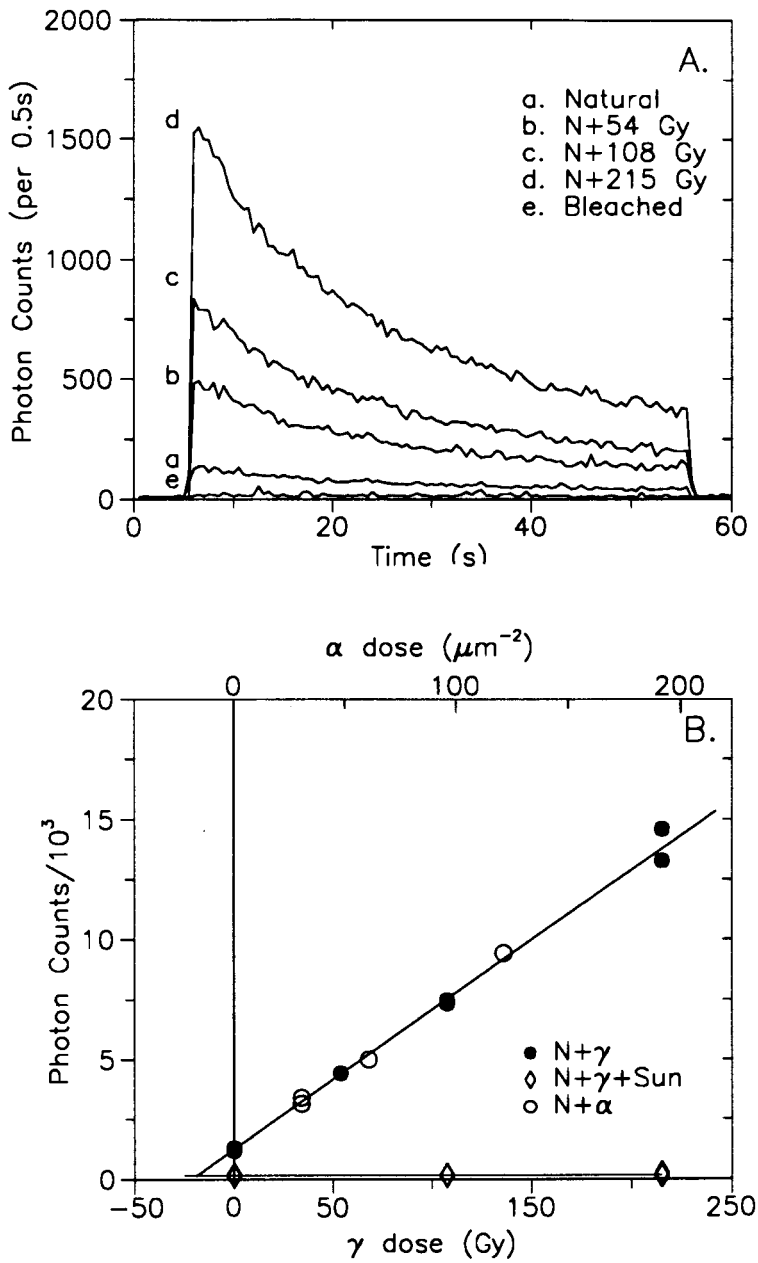

Figure 4.3: Data for LCP5. A. Luminescence decay curves. B. Additive dose data for the first 5 s time interval. Shown is a linear fit to the N+γ and N+α data, and a constant fit to the data for the bleached samples.

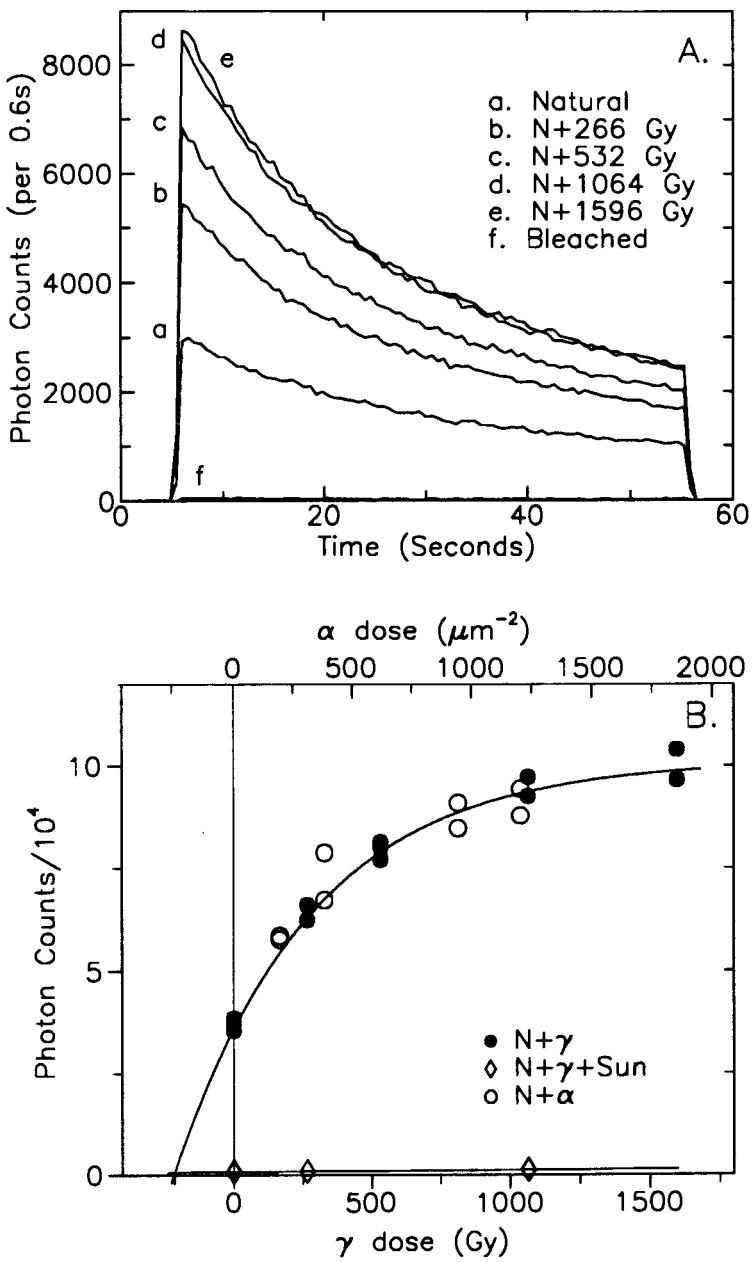

Figure 4.4: Data for MPS1. A. Luminescence decay curves. B. Additive dose data for the first 10 s time interval. Shown is a saturating exponential fit to the N+γ and N+α data, and a linear fit to the data for the bleached samples.

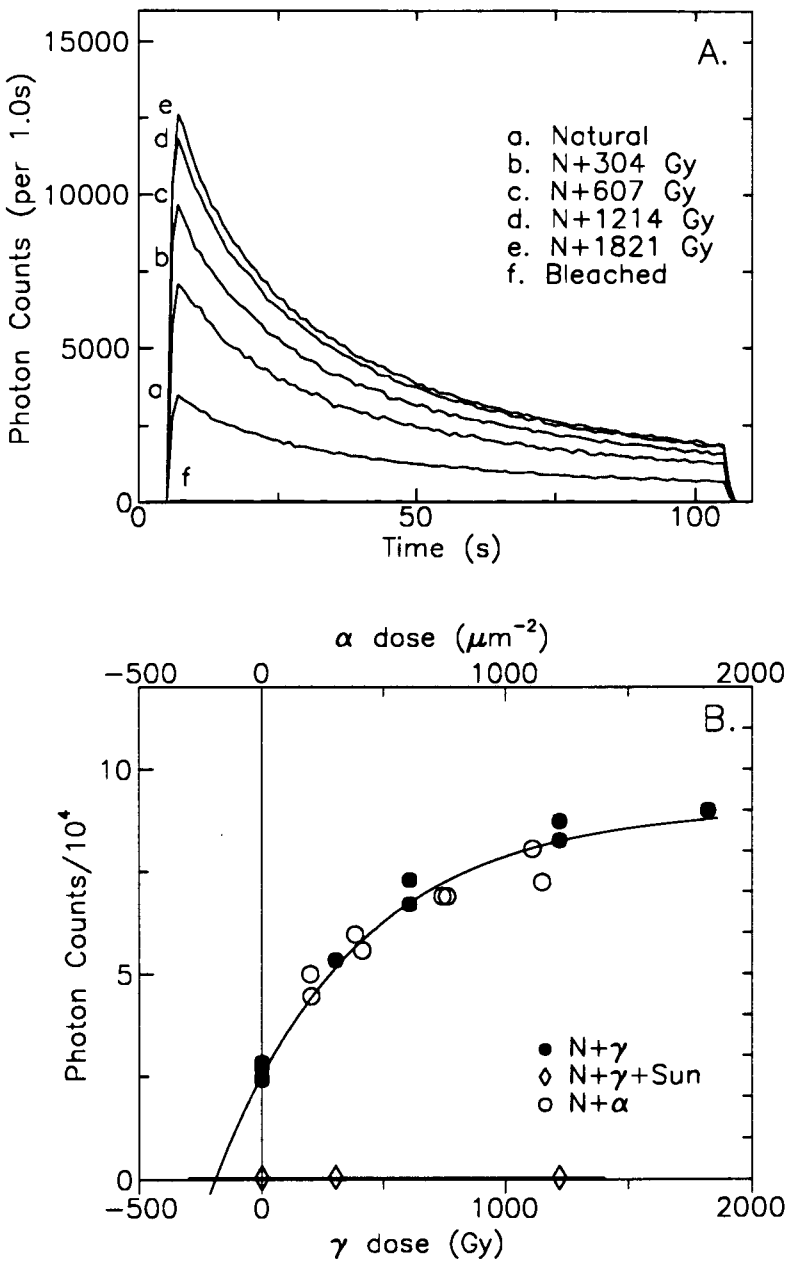

Figure 4.5: Data for MPS2. A. Luminescence decay curves. B. Additive dose data for the first 10 s time interval. Shown is a saturating exponential fit to the N+γ and N+α data, and a constant fit to the data for the bleached samples.

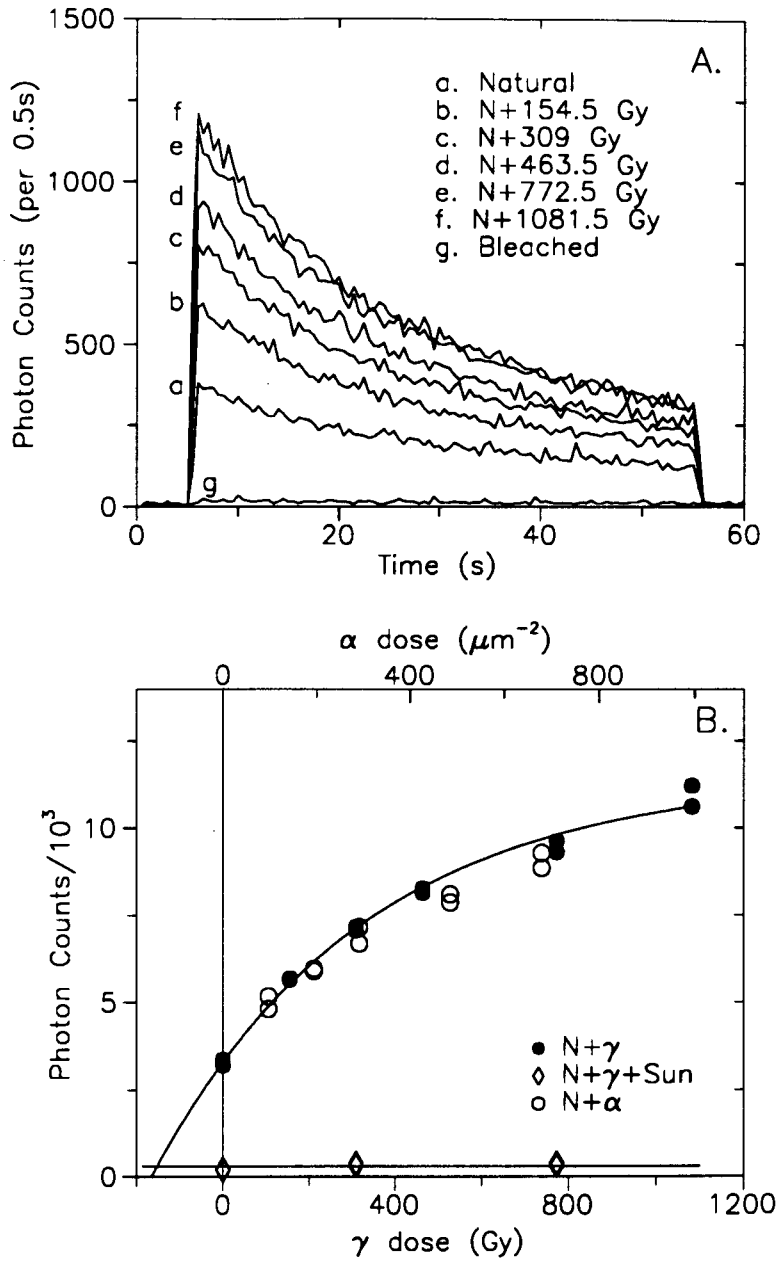

Figure 4.6: Data for WFP1. A. Luminescence decay curves. B. Additive dose data for the first 5 s time interval. Shown is a saturating exponential fit to the N+γ and N+α data, and a constant fit to the data for the bleached samples.

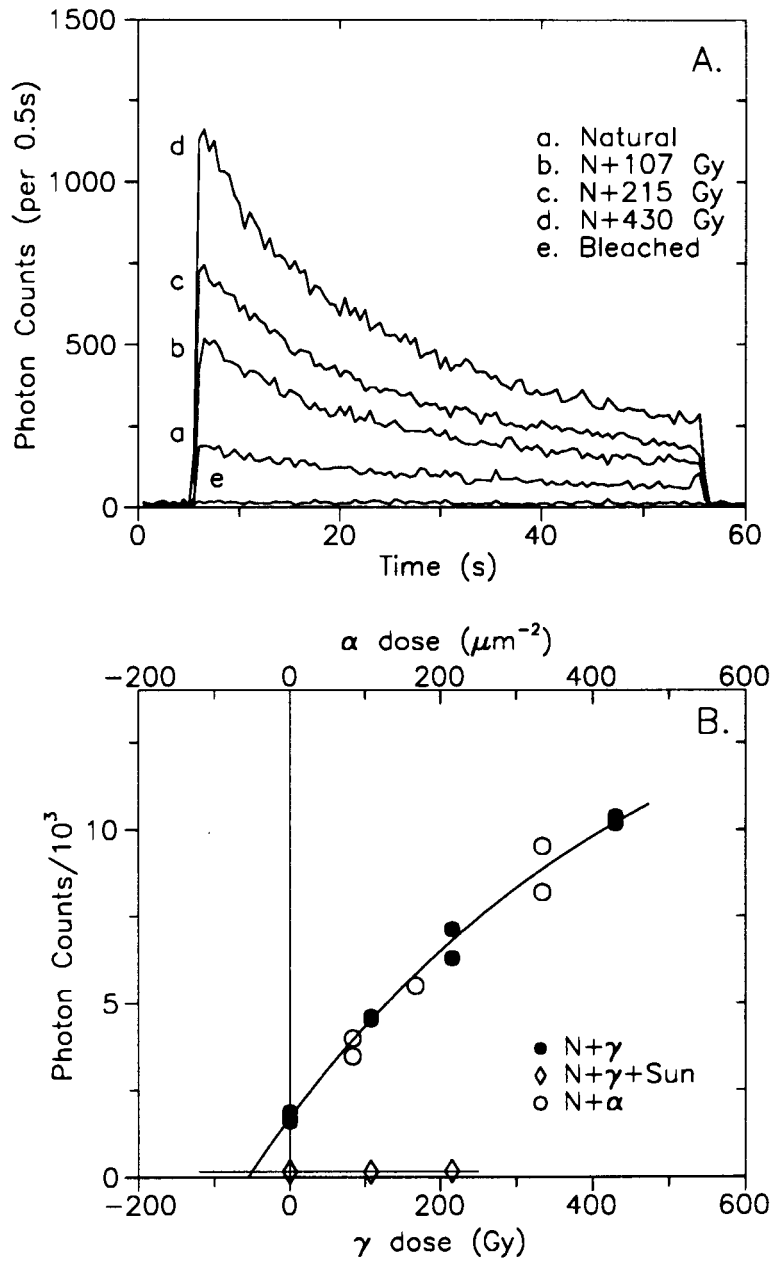

Figure 4.7: Data for WFP2-6. A. Luminescence decay curves. B. Additive dose data for the first 5 s time interval. Shown is a saturating exponential fit to the N+γ and N+α data, and a constant fit to the data for the bleached samples.

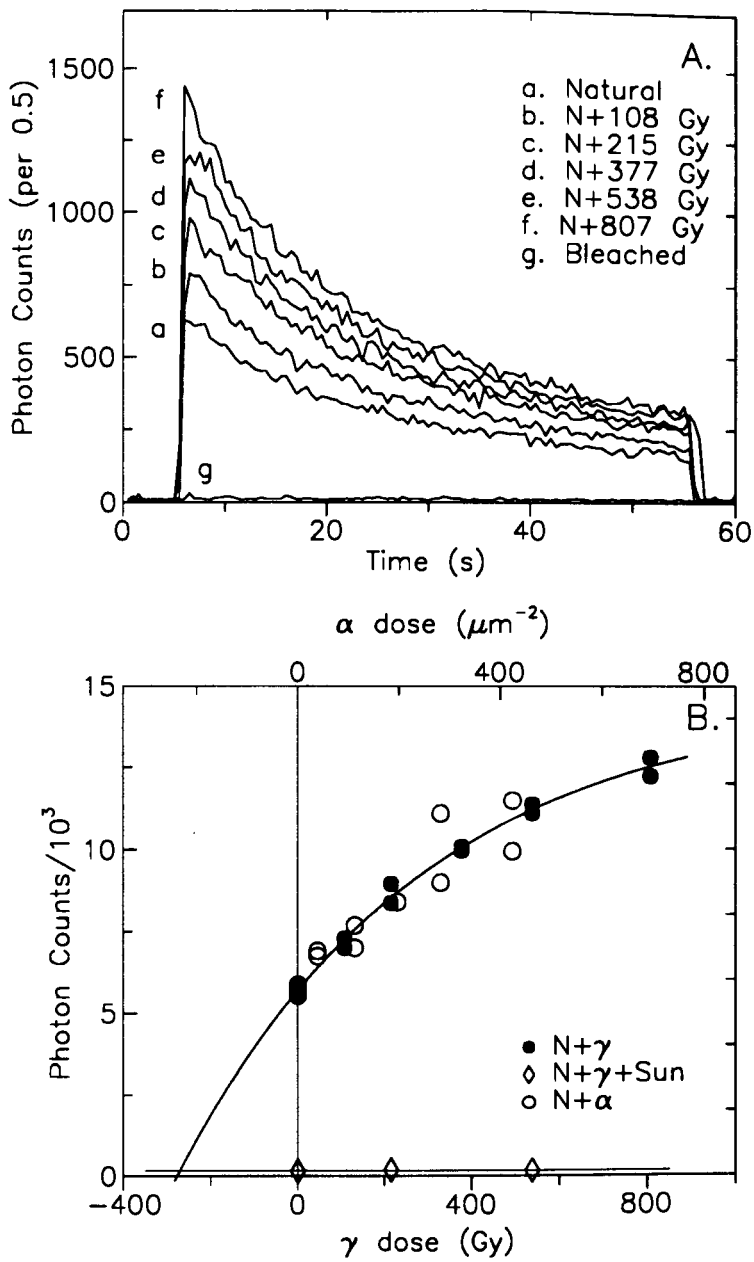

Figure 4.8: Data for SSP2-6. A. Luminescence decay curves. B. Additive dose data for the first 5 s time interval. Shown is a saturating exponential fit to the N+γ and N+α data, and a constant fit to the data for the bleached samples.

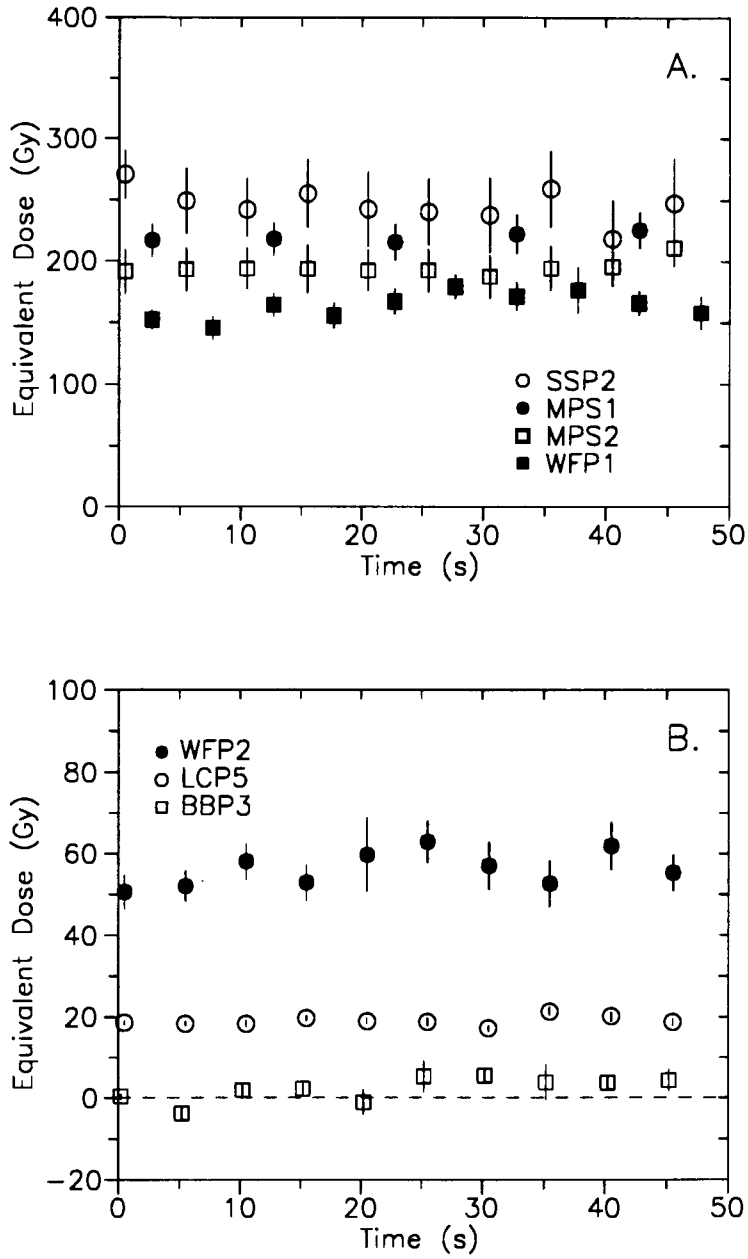

Figure 4.9: Equivalent dose estimates for samples as a function of time after the shutter was opened to allow the infrared diodes to illuminate a sample. Each equivalent dose was calculated using a set of sums of photon counts over a 5 s (10 s for MPS1 and MPS2) interval on the decay curves. Some points have been shifted horizontally a small distance for clarity. The data points for MPS2 have been scaled horizontally by a factor of 2 in order to be fitted in the graph, for these the abscissa should read from 0 to 100 s.

will be discussed later in chapter 6.

It has been observed that the lifetime of trapped electrons in some feldspars is much less than the lifetime predicted by their thermal trap depth. The phenomenon is called *anomalous fading*. Detailed discussions for anomalous fading can be found in Aitken 1985 and Spooner 1993. The amount of anomalous fading depends on the storage time and the storage temperature. The existence of such fading is thought to be related to some quantum tunnelling effects and is still not fully understood (Spooner 1993).

In this work, all samples were heated at 140 ℃ for a week to empty thermally unstable traps in order to avoid the effect of thermal fading, but it is not clear to what extent the anomalous fading component was removed by heating.

2. Initial exposure

All the samples except MPS2 and BBP3 were normalized to correct for the disc to disc variability. The normalization was done by illuminating all the sample discs for a short time, usually one second ($20\,mJ/cm^2$), and measuring the stimulated luminescence. The luminescence intensities obtained were divided by the mean intensity for later use as normalization factors for the sample discs. The initial exposure to infrared light usually does not deplete significantly the population of electron traps and can be ignored in the calculation of equivalent doses. The effect of the initial exposure may be deduced by examining the initial decays on the decay curves of natural sample discs. It was found in this work that such initial exposure caused the stimulated luminescence (photon counts per second) to drop by one to three percent. No corrections for this were made.

3. Preheat

The laboratory radiation can populate not only the deep traps which are thermally stable over a geological time scale, but also shallow traps which do not have a long enough thermal lifetime. It is assumed that by preheating samples after performing the irradiations, these shallow traps are emptied and therefore only those traps which are thermally stable are sampled in luminescence measurements.

Although it is a common practice to heat samples before luminescence measurements, the effect of preheat on the obtained equivalent doses is still not fully investigated so far. Some people still maintain that for infrared optical dating, preheating sample discs is not necessary (Hütt *et al.* 1992, 1993). The argument was based on the thermo-optical model, which is still not finally proven.

The preheat temperature (140℃) was chosen on the basis of the results obtained by Ollerhead *et al.* (1994) and Huntley *et al.* (1993). A temperature independence of equivalent dose values in the range 120℃—160℃ was reported in the these papers. The stimulated luminescence intensity from a sample is usually lower after the preheat than before the preheat, but the extent may differ from sample to sample. The decrease of luminescence for the peat samples selected for this work ranged from about 90% for WFP1 to about 50% for SSP2-6.

4. Bleach

The bleached samples were used to correct for the unwanted thermal transfer of electrons from thermally-stable light-insensitive traps to light-sensitive traps in this work. For some very bright samples, such as MPS1, MPS2 and WFP1, it was found that two to three hours of bleach did not empty all the light-sensitive traps, especially for samples with longer laboratory irradiation times. The incomplete bleaching of light-sensitive traps may result in an underestimate of the equivalent doses, but on the other hand, considering the brightness of the natural sample discs compared to the bleached ones, this effect can be safely neglected.

Chapter 5

Dose-rate Evaluations

The natural dose experienced by sediments mainly comes from α, β and γ rays emitted by radioactive substances both in the sediments to be analyzed and in the surroundings. There is also a small contribution from cosmic radiation. The main contributors to the dose rate are isotopes of uranium, thorium and potassium, *i.e.*, ^{238}U, ^{232}Th, ^{40}K and their decay products. Decay chains of these isotopes can be found in Aitken (1985). Evaluation of the dose rate thus involves a calculation of each individual contribution.

Dose rates from uranium, thorium and potassium can be calculated directly from the contents of the isotopes in a sediment sample. Because water and organic materials were also present in the sediments and they absorb the radiation energy differently than the mineral matter, the dose rate must be corrected for their presence.

The cosmic radiation dose rate varies with depth of burial and has varied since each sediment was buried at different depths for different times. The total past dose from cosmic rays, therefore, was estimated (see section 5.4) instead of calculating the dose rate as is conventional.

Table 5.1: Water and organic material contents

Sample	Δ^w (*in situ*)	Δ^w (saturated)	Δ^o
LCP5	3.60	3.80	1.68
MPS1	0.307	0.350	0.067
MPS2	0.436	0.482	0.125
WFP1	0.693	0.895	0.547
WFP2-6	0.677	1.91	1.30
SSP2-6	1.23	2.05	1.20

5.1 Water & organic material contents

Peat samples may be considered to consist of three components: mineral, organics, and water. The contents of water and organics are defined here as follows:

$$\Delta^w = \frac{\text{mass of water}}{\text{mass of minerals}} \tag{5.1}$$

$$\Delta^o = \frac{\text{mass of organics}}{\text{mass of minerals}} \tag{5.2}$$

Water contents and organic material contents were measured for all samples studied (performed by G. Morariu) and are listed in table 5.1. Because the peat samples were probably under water for most of the time in the past (*e.g.*, when covered by ice or thick sediments, the peat samples would have been below the water table), the water contents were likely to have been close to saturation. Saturated water contents were therefore used for dose rate calculations. The uncertainties of all measured water contents in table 5.1 were assumed to be 5% since no such information was available.

5.2 U, Th, K contents and γ-spectrometry

The contents of uranium, thorium and potassium were obtained in order to calculate dose rates. Uranium contents were measured using delayed neutron analysis[1].

[1] Australian Nuclear Science & Technology Organization, Private Mail Bag 1, Menai, NSW 2234, Australia.

Table 5.2: U, Th and K contents

Sample	C_U (μg/g)	C_{Th} (μg/g)	C_K (%)†
LCP5	1.26 ± 0.09	1.9 ± 0.1	0.76
MPS1	1.90 ± 0.11	4.5 ± 0.2	1.05
MPS2	2.55 ± 0.13	4.4 ± 0.2	0.91
WFP1	1.71 ± 0.10	5.5 ± 0.2	1.35
WFP2-6	0.35 ± 0.05	(≤ 0.19*)	0.16
SSP2-6	0.68 ± 0.06	2.0 ± 0.1	0.25

* Estimated value using the data of another sample nearby.

†Accuracy estimated to be 5%.

Thorium contents were obtained through neutron activation analysis[2]. Potassium contents were analyzed using atomic absorption spectroscopy[3]. The results are listed in table 5.2. Dried and milled substances were used for these analyses. The uncertainties for all potassium contents were not available and therefore a 5% uncertainty was assumed for all.

The average ranges of α, β and γ radiation from natural radioactivity in soil are about 25 μm, 2 mm and 45 cm, respectively (Divigalpitiya 1982). Hence, the total dose received by a bulk sample is actually from two contributions: 1) the α and β doses from radioisotopes within the bulk sample since the ranges of α and β particles are relatively small; and 2) the γ dose mainly from radioisotopes in the surroundings. The U, Th and K contents can be used for the calculation of α and β dose rates because of the ranges of these particles. But the γ dose rate may be underestimated if these contents are used for the calculation, because the peat is not infinitely thick and the surroundings generally have higher U, Th and K contents.

In addition, *in situ* γ dose rates ($\dot{D}'_\gamma$) were also measured with a portable NaI

[2]SLOWPOKE Reactor Facility,University of Toronto, Canada M5S 1A4.

[3]Chemex Labs Ltd., 212 Brooksbank Ave., North Vancouver, B.C., Canada, V7J 2C1.

Table 5.3: γ-spectrometry results

Sample	$\dot{D}'_\gamma$ (Gy/ka)	C_U (μg/g)	C_{Th} (μg/g)	C_K (%)
LCP5	0.230 ± 0.013	0.73 ± 0.09	1.48 ± 0.12	0.34 ± 0.02
MPS1	0.554 ± 0.019	1.73 ± 0.14	3.37 ± 0.21	0.88 ± 0.03
MPS2	0.562 ± 0.019	2.12 ± 0.14	2.98 ± 0.19	0.78 ± 0.03
WFP1	0.426 ± 0.016	1.24 ± 0.12	2.75 ± 0.17	0.73 ± 0.02
WFP2-6*	0.110 ± 0.009	0.36 ± 0.07	0.88 ± 0.10	0.17 ± 0.01

* The probe was not inserted deep enough for these values to be considered reliable.

γ-spectrometer[4]. $\dot{D}'_\gamma$ is deduced from the count rate of γ rays in the range 0.85—2.7 MeV on the assumption of secular equilibrium. The U, Th and K contents can also be calculated from the area of the γ peaks corresponding to each of the elements. These should be regarded as "apparent contents" as they will only be the actual ones if the material is homogeneous to at least 50 cm from the probe in all directions, and in secular equilibrium. The results are listed in table 5.3.

The γ-spectrometer usually overestimates the γ dose rate from the surroundings because it does not measure the low energy γ rays. The actual γ dose rate, therefore, should lie between the γ dose rate given by the γ spectrometer and the γ dose rate calculated using analyzed U, Th and K contents.

5.3 U, Th and K dose-rate calculation

The total dose rate was determined separately for these two contributions mentioned above. The corrections of dose rates due to water and organic contents were carried out using Δ values of each sample following the argument of Divigalpitiya (1982).

The U, Th and K contents listed in table 5.2 were used to calculate the contributions from α and β radiation from within the sample. The dose rates are given by

[4]GR-256, manufactured by Explorium G.S. Limited, 55 Healey Road, Bolton (Toronto), Ontario, L7E 5A2.

Table 5.4: Values of H, d, and r coefficients*

i	H_{iw}	H_{io}	r_{iU}	r_{iTh}	d_{iK}
α	1.50	1.37	—	—	—
β	1.25	1.2	0.147	0.0286	0.815
γ	1.14	1.1	0.1136	0.0521	0.243

*The d values are dose rates (Gy/ka) per 1% K; the r values are dose rates (Gy/ka) per μg/g of U or Th.

(Aitken 1985, Berger 1988):

$$\dot{D}_\alpha = 4\eta(k_U\frac{C_U}{0.82} + k_{Th}\frac{C_{Th}}{0.85})b\frac{1+\Delta^o}{1+H_{\alpha o}\Delta^o + H_{\alpha w}\Delta^w} \quad (5.3)$$

$$\dot{D}_\beta = (d_{\beta K}C_K + r_{\beta Th}C_{Th} + r_{\beta U}C_U)\frac{1+\Delta^o}{1+H_{\beta o}\Delta^o + H_{\beta w}\Delta^w} \quad (5.4)$$

$$\dot{D}_\gamma = (d_{\gamma K}C_K + r_{\gamma Th}C_{Th} + r_{\gamma U}C_U)\frac{1+\Delta^o}{1+H_{\gamma o}\Delta^o + H_{\gamma w}\Delta^w} \quad (5.5)$$

where:

—$\dot{D}_i$'s are dose rates;

—C_U, C_{Th} and C_K are U, Th and K contents, respectively;

—η is a constant and equal to 0.9 (Aitken and Bowman 1975);

—k_U and k_{Th} are thick-source α count rates per unit area, $k_U = 0.128\,\mathrm{ks^{-1}\,cm^{-2}}$ per μg/g U, $k_{Th} = 0.0372\,\mathrm{ks^{-1}\,cm^{-2}}$ per μg/g Th (Huntley *et al.* 1986);

—$H_{\alpha w}$ and $H_{\beta w}$ (or $H_{\alpha o}$ and $H_{\beta o}$) are the ratios of specific stopping powers of water (or organics) to dry sediment for α and β particles, respectively;

—$H_{\gamma w}$ (or $H_{\gamma o}$) is the ratio of absorption coefficient of water (or organics) to dry sediment for γ radiation.

The H, d and r coefficients used for calculation are listed in table 5.4; H_{iw} from Aitken (1985), $H_{\alpha o}$ and $H_{\beta o}$ from Divigalpitiya (1982), $H_{\gamma o}$ is chosen on the basis of the argument of Aitken and Xie (1990) for $H_{\gamma w}$; r_{ij} from Nambi and Aitken (1986); d_{ij} from Berger (1988).

Table 5.5: Calculated dose rates

Sample	$\dot{D}_\alpha$	$\dot{D}_\beta$	$\dot{D}_\gamma$	$\dot{D}'_\gamma$	$\dot{D}$
LCP5	0.08 ± 0.01	0.30 ± 0.03	0.16 ± 0.02	0.230 ± 0.013	$\mathbf{0.57 \pm 0.03}$
MPS1	0.43 ± 0.05	0.89 ± 0.04	0.51 ± 0.02	0.554 ± 0.019	$\mathbf{1.84 \pm 0.06}$
MPS2	0.40 ± 0.04	0.80 ± 0.03	0.49 ± 0.02	0.562 ± 0.019	$\mathbf{1.72 \pm 0.06}$
WFP1	0.23 ± 0.03	0.84 ± 0.05	0.48 ± 0.02	0.426 ± 0.016	$\mathbf{1.50 \pm 0.06}$
WFP2-6	0.03 ± 0.01	0.09 ± 0.01	0.04 ± 0.01	0.110 ± 0.009	$\mathbf{0.18 \pm 0.01}$
SSP2-6	0.07 ± 0.02	0.16 ± 0.01	0.11 ± 0.01	—	$\mathbf{0.34 \pm 0.02}^*$

*$\dot{D}_\gamma$ value was used in the place $\dot{D}'_\gamma$ since the latter was not measured.

When used for calculating the dose rates, the measured $\dot{D}'_\gamma$ values must be corrected for the water contents because the latter was not in saturation at the time of the measurement. The correction can be done as follows:

$$\dot{D}'_{\gamma c} = \dot{D}'_\gamma \frac{1 + H_{\gamma w}\Delta^w_{in\ situ} + H_{\gamma o}\Delta^o}{1 + H_{\gamma w}\Delta^w_{saturated} + H_{\gamma o}\Delta^o} \tag{5.6}$$

The obtained $\dot{D}_\gamma$ and $\dot{D}'_{\gamma c}$ represent the two extreme cases of the total γ dose rate: the former is the γ dose rate from within the grains, while the latter from the surroundings. Therefore, the average of $\dot{D}_\gamma$ and $\dot{D}'_{\gamma c}$ was used for the γ dose rate, and the standard deviation was taken as $\frac{1}{4}(\dot{D}_\gamma - \dot{D}'_{\gamma c})$. The total dose rate $\dot{D}_{\alpha\beta\gamma}$ (excluding the cosmic ray contribution) is, therefore:

$$\dot{D} = \dot{D}_\alpha + \dot{D}_\beta + \frac{1}{2}(\dot{D}_\gamma + \dot{D}'_{\gamma c}) \tag{5.7}$$

The calculated dose rates for each sample are shown in table 5.5.

5.4 Cosmic radiation dose estimates

The cosmic-ray dose rate delivered to "standard rocks" as a function of depth below ground level at a geomagnetic latitude of 55° was given as (Prescott and Hutton 1994 using data from Barbouti and Rastin 1983):

$$\dot{D}_c = \frac{C}{((x+d)^\alpha + a)(x+H)} \exp(-Bx) \tag{5.8}$$

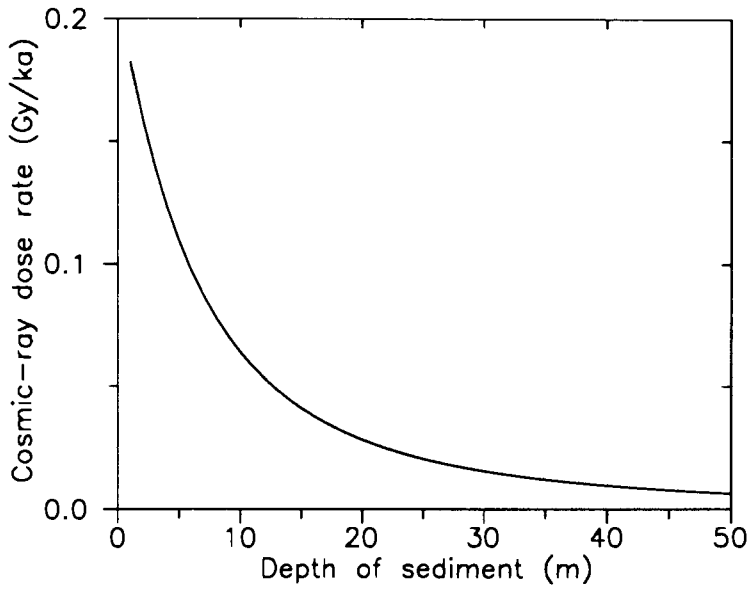

Figure 5.1: Cosmic ray dose rates *vs.* depth. The mass density of sediments was taken to be $2\,g/cm^3$.

where, $\dot{D}_c$ is in Gy/ka, x is the depth of a sediment below ground level (in hg/cm^2 or $100\,g/cm^2$), $C = 6072$, $B = 5.50 \times 10^{-4}$, $d = 11.6$, $\alpha = 1.68$, $a = 7.5$ and $H = 212$. This expression is valid for x from $1.5\,hg/cm^2$ (at which the 'soft parts' of cosmic rays, mainly electrons, are absorbed completely) to $10^4\,hg/cm^2$. This relationship for cosmic-ray dose rate and depth is shown in figure 5.1 (the density was taken to be $2\,g/cm^3$ in all the calculations). The cosmic-ray dose rate is about 0.28 Gy/ka at the surface if the soft parts of cosmic rays are taken into account (Aitken 1985).

The buried depth of sediments varied drastically in the past, for example, during a glacial age, sediments could have been covered by ~1 km of ice. The cosmic-ray dose rate was thus far from constant in any sense. A range of possible values of the cosmic-ray dose for each sample was therefore estimated by considering the different possible histories of the sediments as follows:

LCP5 This sample was formed about 33 ka ago (^{14}C age). It was covered by fluvial silt (minimum ~20 cm) at 25 ka or earlier. The cosmic-ray dose rate from 33 to 25 ka probably lies in the range 0.1—0.25 Gy/ka resulting in a dose from 0.8

to 2 Gy. Between 25 and 22 ka, about 10 m of Quadra sand was deposited on top, and the cosmic-ray dose rate was about 0—0.05 Gy/ka (dose 0—0.2 Gy). Between 22—5 ka, there was additionally a lake , ice (>1 km) and/or sediment (~70 m thick), and the dose rate during this time was negligible. In the last 5 ka, the peat was a few meters below the ground level as it is now (~2m, dose rate 0.15 Gy/ka, dose 0.75 Gy). From this, the total cosmic-ray dose is probably in the range 1.55—2.95 Gy. Setting this range to cover two standard deviations, the total cosmic-ray dose is then 2.2 ± 0.4 Gy.

MPS1 This sample was formed about 100 ka ago. For the first 10 ka, it was buried 0—11 m below the ground level (dose rate 0.1—0.25 Gy/ka, dose 1—2.5 Gy). For the next 80 ka, it was 11—26 m below the ground level (dose rate 0.02—0.1, dose 1.6—8 Gy). For the last 20 ka it probably stayed at 26 m below the ground level as it is now (dose rate<0.02 Gy/ka, dose 0—0.4 Gy). The total cosmic-ray dose for this sample is about 2.6—11 Gy. The total cosmic-ray dose is taken to be 6 ± 2 Gy.

MPS2 This sample is quite similar to MPS1 and the arguments for MPS1 are also applicable to this sample. The cosmic-ray dose is thus taken to be 6 ± 2 Gy.

WFP1 This sample is 7 m below WFP2-6. The total cosmic-ray dose for this sample is probably similar to that of WFP2-6 (discussed below, cosmic-ray dose 2 ± 1 Gy).

WFP2-6 This sample could have stayed at the ground level for the first 10 ka (dose rate 0.25 Gy/ka, dose 2.5 Gy). Then it was buried 25 m below ground level (dose rate <0.02 Gy/ka, dose <2 Gy). The total cosmic-ray dose is thus about 0—4 Gy and is estimated to be 2 ± 1 Gy.

SSP2-6 This sample is located 150 m below the top of the valley. Assume that in the first 15 ka it was 1 m below the ground level, the cosmic-ray dose would be 3 Gy (dose rate ~0.2 Gy/ka). Considering it was buried then at 40 m for 750 ka, the cosmic-ray dose could be 7.5 Gy (dose rate <0.01 Gy/ka). The total cosmic-ray dose is then 6 ± 2 Gy.

Chapter 6

Optical Ages

6.1 Optical ages

The ages of the peat samples were calculated using the age equation discussed in section 1.1 (equation(1.2)) as well as the data given in the previous chapters. The calculated ages are listed in table 6.1. For optical dating, the ages obtained normally correspond to the time elapsed since the sediments were last exposed to sunlight. In the case of peat, the dose rate used for the calculation is that appropriate to compacted peat. There is a period of time between deposition and compaction when the dose rate is much lower. The ages in this case are better described as the time since compaction by the overlying sediments.

6.2 Discussion

The main objective of this work was to determine whether or not the infrared optical dating technique would yield correct ages for sediments of known ages or unknown ages but with restrictions. The obtained ages in table 6.1 did show such a consistency. The following is a discussion of the results.

BBP3 This sample was very young and was expected to yield a zero age. The equivalent dose obtained for it was 0 ± 1 Gy and was consistent with zero. This

Table 6.1: Calculated ages

sample	D_e (Gy)	D_c (Gy)	$\dot{D}$ (Gy/ka)	age (ka)
BBP3	0 ± 1	—	0.5 (assumed)	0 ± 2
LCP5	19 ± 1	2.2 ± 0.4	0.57 ± 0.03	29 ± 2
MPS1	218 ± 13	6 ± 2	1.84 ± 0.06	115 ± 8
MPS2	194 ± 17	6 ± 2	1.72 ± 0.06	109 ± 11
WFP1	164 ± 8	2 ± 1	1.50 ± 0.06	108 ± 7
WFP2-6	56 ± 5	2 ± 1	0.18 ± 0.01	—
SSP2-6	246 ± 30	6 ± 2	0.34 ± 0.02	706 ± 98

indicates that its mineral grains were well exposed to sunlight at the time of deposition. In a sense of consistency, it is necessary for zero age sample to give a zero equivalent dose in order to make the ages for older samples more believable. From the result, it is clear that this condition is satisfied.

LCP5 The age obtained for this sample was 29 ± 2 ka while the ^{14}C age was 35 ka (~39 ka when corrected to calendar years; see Bard *et al.* 1990). The discrepancy may be explained if the depositional circumstances are considered. Peat was present as an active bog at first, and the main constituent was water. During this time, the dose rate was mainly determined by the contribution from cosmic rays (about 0.2 Gy/ka). The dose rate obtained in chapter 5 was valid only for the period after the compaction of peat by sediments deposited before the subsequent glaciation. Based on the radiocarbon ages of the valley fill in adjacent Seymour Valley (*i.e.*, the time when the valley was filled by ice during a glacial age, Lian and Hickin 1993), compaction of LCP5 would have occurred shortly after 29 ka (^{14}C age, ~33 ka in calendar years) and certainly not after 22 ka (^{14}C age, ~25 ka in calendar years). The obtained age for LCP5 is consistent with this range for the time of compaction.

MPS1, MPS2 The optical dating ages for these samples are 115 ± 8 ka for MPS1 and 109 ± 11 ka for MPS2. Since these samples are organic-rich sediments, they were deposited definitely during a nonglacial period. The pollen shows that

these were deposited in interglacial periods, either about 120 ka or about 240 ka ago (δ^{18}O stage 5 or 7). The ages obtained are consistent with deposition during the last interglacial period.

WFP1, WFP2-6 The optical dating age for WFP1 (108 ± 7 ka) supports the previous suggestion that the Whidbey Formation is correlated with the Muir Point Formation. This sample was also an organic-rich sediment and the dating result did lie within the last interglacial period as expected. The age of WFP2-6 was not calculated because the equivalent doses obtained for different parts of the same bulk sample WFP2 were different (D.J. Huntley, private communication), and this could not be accounted for by inhomogeneities. It is possible that this resulted from that fact that the sample collected from the face of the peat bed was very friable, allowing radioactive elements and sediments from overlying exposures to wash through. Sampling further into the face may overcome this.

SSP2-6 This sample was selected as a test of optical dating method on a very old sample. The optical age for this sample is related to the time of compaction by overlying material as in the case of LCP5. The obtained age for this sample was 706 ± 98 ka. This is consistent with the expected age of just under 780 ka if the magnetic reversal is the Brunhes-Matuyama. If, on the other hand, the reversal is that at the end of the Jaramillo at 1.06 Ma, then the age obtained is too young. Since the latter seems the more likely, a calculation for the effect of thermal fading is presented below. If thermal fading cannot be ignored in this case, then the age obtained will definitely be too young and thus unreliable. This can not be solved unless there is more information known about the things such as the age, the thermal lifetime, *etc.*.

6.3 Thermal fading

In section 4.2, the equivalent doses were obtained without considering the possible existence of thermal fading. This may cause the obtained ages for very old samples to be younger than they should be. The effect of thermal fading is discussed here

by considering a single-trap model. If n is the density of trapped electrons and N is the trap density, the rate for filling the traps can be approximately described by the following equation (Chen and Kirsh 1981, p.26):

$$\frac{dn}{dt} = \frac{N-n}{\tau_0} - \frac{n}{\tau} \tag{6.1}$$

where the first term describes the filling of traps, and the second term describes the thermal eviction, with τ the thermal lifetime of trapped charge carriers, and τ_0 a constant related to the filling of traps and which incorporates the dose rate.

The boundary condition for equation 6.1 is that for $t \rightarrow \infty$, dn/dt will approach zero, because the two competing process, *i.e.*, the filling and the emptying of traps, will reach equilibrium given sufficient time. Assuming that at $t = 0$, $n = 0$, the solution for equation(6.1) is:

$$n = \frac{N}{1+\frac{\tau_0}{\tau}}(1 - e^{-(\frac{1}{\tau}+\frac{1}{\tau_0})t}) \tag{6.2}$$

If the decay due to a finite thermal lifetime of traps does not exist, *i.e.* $\tau \rightarrow \infty$, the solution would be a saturating exponential as is used in chapter 4 for the fitting of experimental data:

$$n = N(1 - e^{-t/\tau_0}) \tag{6.3}$$

If luminescence intensity is linearly proportional to the density of trapped charge carriers, as from equation(6.3), then we have:

$$\frac{I}{I_0} = \frac{n}{N} = (1 - e^{-\dot{D}t/D_0}) \tag{6.4}$$

where I is the luminescence intensity for a natural and I_0 is the saturation intensity. It is clear that the parameter τ_0 can be determined from the dose rate $\dot{D}$ and the fitting parameter D_0:

$$\tau_0 = D_0/\dot{D} \tag{6.5}$$

Values for the samples are given in table 6.3.

If the age for sample SSP2-6 is actually 1.06 Ma as suggested by other studies (see chapter 3), then from the parameters obtained, the thermal lifetime τ is deduced to be 2500 ka. Assuming that this thermal lifetime is applicable to the other samples, the ages can be corrected. The results are listed in table 6.3.

Table 6.2: Calculated ages for $\tau = 2500$ ka*

sample	D_0 (Gy)	I/I_0	τ_0 (ka)	age (ka)
MPS1	498	0.406	270	140
MPS2	591	0.285	344	115
WFP1	488	0.284	325	109
WFP2-6	527	0.101	2928	—
SSP2-6	566	0.393	1664	1060

* All D_0's and I/I_0's are from the fits shown in figures 4.4—4.8 for the first 5 s or 10 s time interval

6.4 Suggestions for future work

From the above results, it is clear that the method used in this work can yield correct ages for young samples ($<\sim$ 100 ka). For the older sample, SSP2-6, the age obtained may be too young as a result of thermal fading. The problem may be solved by investigating the thermal lifetime, or the trap depth of trapped electrons in feldspar samples. A better understanding of the physical processes for infrared optical dating is also required.

The simple model in section 6.3 may also provide a possible way to correct for the thermal fading if the fading exists. The thermal lifetime of a feldspar sample may also be determined by comparing the actual age and the optical age of a known-age sample. Further investigations are necessary to confirm this model.

It is not known whether or not disequilibrium existed in the decay chains of ^{238}U and ^{232}Th in the samples selected for this work. This is ignored in all the dose rate calculations. Further studies are needed on the possible effects of disequilibrium in the decay chains.

Chapter 7

Conclusions

From the dating results for samples selected for this work, it appears that optical dating of organic-rich sediments using 1.4 eV infrared light can produce satisfactory ages for sediments with ages between 0 and about 100 ka.

The optical age for a modern peat (BBP3) is consistent with zero. The age obtained for LCP5 is in good agreement with the accepted age. The optical ages for WFP1, MPS1 and MPS2 are consistent with the fact that they were formed during the last interglacial period, and provide strong confidence that they were not formed during an earlier interglacial.

The result for SSP2 suggests that the method may be applied to sediments with ages up to 800 ka. Further studies are necessary to confirm this.

It was found that inhomogeneities in these types of sediments can be very large as in the case of WFP2. Samples should be examined for homogeneity to prevent giving questionable dating results.

Appendix A

Sample Preparation

A.1 Fine-grain sample preparation

Fine-grain sample preparation (Divigalpitiya 1982, Lian 1991) was used on peat samples. The procedure includes the following steps (all steps were performed in the dark room with minimum red light illumination):

1. The outer surfaces of peat blocks sampled from the field were removed. This is to exclude materials which had been exposed to sunlight at the time of collection.
2. The peats blocks were shaved to small bits and were examined for small sand bed. Small sand beds were scraped off if they were found. This was done to exclude any sediments which had been deposited by fluvial processes.
3. The small peat bits were then left in distilled water for about a day. After this, the peat would expand and loosen up.
4. 10% hydrogen peroxide was added to the peat to remove organics. The H_2O_2 solution was replaced daily. This procedure lasted for three or four days until the reaction between H_2O_2 and organic materials had stopped.
5. The sample was wet-sieved through a 210 μm nylon mesh, and then left to settle for four hours. The water was decanted after this.
6. The sample was treated for two hours with 10% HCl to dissolve any carbonates present; the sample was then rinsed with distilled water.

7. The sample was put in 100 ml citrate bicarbonate dithionate (CBD) for 12 hours. This was done to remove any luminescence-blocking iron oxide coatings on the sediment grains. The CBD solution was made by adding 71 grams of citrate, 8.5 grams of bicarbonate, and 2 grams of dithionate to a litre of distilled water.
8. Stokes settling in a 20 cm column of 1 gram/litre Calgon solution for 30 minutes (suspension saved) and then for 4 hours (suspension discarded). The Calgon is needed to deflocculate any clay present.
9. Stokes settling in a 20 cm column of distilled water for 3 to 4 hours (suspension discarded) followed by three 30 minute settlings (suspension saved). This procedure selected 4 to 11 μm grains.

A.2 Coarse-grain sample preparation

Feldspar and quartz grains were extracted from bulk sediments using a coarse-grain sample preparation technique. The first few steps were to separate selected-size quartz and feldspar grains:

1. 10% HCl treatment to remove carbonates.
2. Dry sieving through 90, 125, 150, 180, 250 μm mesh screens.
3. Density separation for selected-size grains using 2.59 g/cm^3 NapT[1] solution. Ideally, the fraction with specific gravity <2.59 g/cm^3 contained alkali feldspars, while the the fraction with specific gravity >2.59 g/cm^3 contained quartz and other feldspars.

The quartz and feldspar grains were then prepared separately for future use:

4. Feldspar preparation (<2.59 g/cm^3)
   1) 10% HF solution etching for six minutes to remove outer layer from all feldspar grains.
   2) 30 min in 10% HCl to prevent fluorides from precipitating; the grains were then wet sieved through a 125 μm mesh screen to remove fragmentary grains.

[1] sodium polytungstate, $Na_2WO_4 \cdot 9WO_3 \cdot H_2O$

3) Rinse the grains thoroughly using distilled water, methanol, and acetone.

4) Magnetic separation using a Franz magnetic separator, angles set at 20° forward, +8° side, coil current set to maximum.

5. Quartz preparation (>2.59 g/cm^3)

1) 40 min in 48% HF solution to etch away the outer 10 μm from all quartz grains and dissolve all feldspars.

2) and 4): Same as step 2)—4) for feldspar preparation.

5) Density separation using 2.69g/cm^3 NapT solution to remove zircons, since a small proportion of zircon can dominate the luminescence (Huntley *et al.* 1988).

Appendix B

The Diring Yuriakh Sample

B.1 Diring Yuriakh Sediments

During the excavations at Diring Yuriakh (Deep Creek) on the Lena River, 140 km upstream from Yakutsk, Siberia, Russia, a Paleolithic stone tool assemblage was discovered. The geographic location of the site was 61° 12′ north latitude, and 128° 28′ east longitude. The stratigraphic section of the site is shown in figure B.1 (after Mochanov 1988). Paleolithic stone tools were found at layer 5, which consists mainly of deflated gravels and pebbles.

Because no fossilized animal or plant remains were found, the stone tool site could not be correlated to any other securely dated site. A paleomagnetic reversal found in layer 8 indicates that these artifacts might be older than Brunhes-Matuyama boundary (780 ka).

Other methods that could give an age for these stone tools are thermoluminescence and optical dating by dating the sands surrounding the artifacts. This work is an attempt to use infrared optical dating to find an upper limit for the age of the stone tools.

The sample selected for this work was taken from layer 3, just below the artifact layer. This layer contains ferruginated, heavy- to medium-grained sands (Mochanov 1988). It was expected that an upper age limit for the stone tools could be obtained by measuring the age of the sand which was deposited before the time when the stone

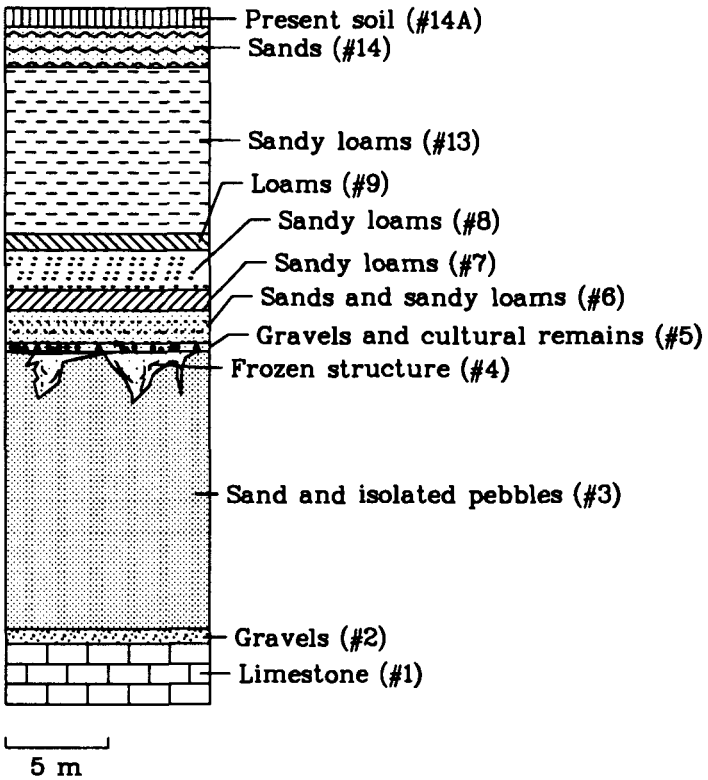

Figure B.1: Diring Yuriakh sample site section. The layers were numbered from #1 to #14A as indicated. Frozen structures similar to that in layer #4 were also found in layer #6 to #14.

tools were made. This can be accomplished if the sands were exposed to light at about the time of deposition.

Quartz and feldspars were extracted from the sample using the coarse-grain preparation procedure (see Appendix A). 1 cm-diameter aluminum planchets were used to hold a portion (10 or 20 mg) of feldspars or quartz for handling. A layer of oil was placed at the bottom of each planchet to prevent the grains from moving.

B.2 Regeneration method

In this method, a set of identical natural samples are first bleached and then are given various radiation doses to regenerate a luminescence growth curve (N+sun+γ). A set

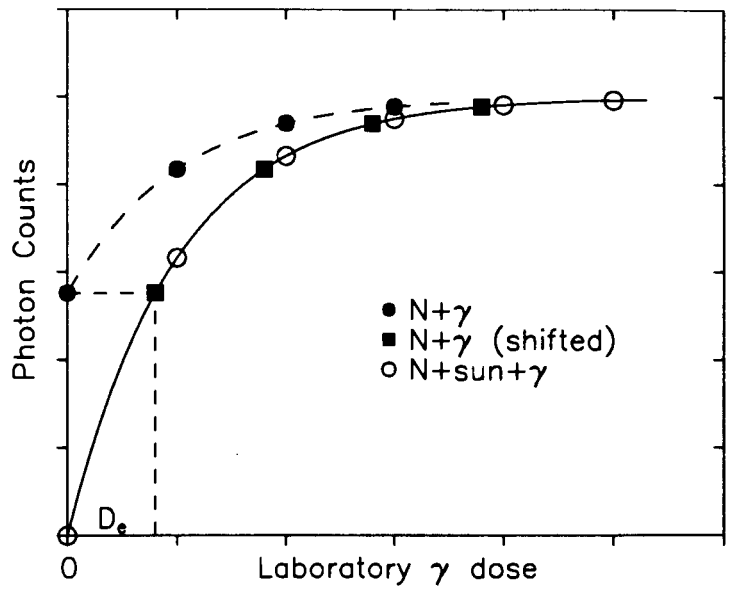

Figure B.2: Regeneration method. The equivalent dose D_e is determined by shifting the fitted curve of (N+γ) data to lay on the regenerated growth curve (N+sun+γ).

of natural and irradiated samples (N+γ) are also prepared to construct an additive dose growth curve. The two growth curves are then compared to deduce an equivalent dose for the natural sample, as shown in figure B.2. This method yields believable results only if the N+γ and N+sun+γ data can be shifted to form a single curve. The method is especially useful when the luminescence for a natural sample approaches saturation and it becomes difficult to extrapolate the N+γ data alone to obtain an equivalent dose.

B.3 Feldspar extracts

The regeneration method was used to determine the equivalent dose of the sample of layer 3 collected from the Diring Yuriakh site. It was observed in a pilot experiment that the luminescence of natural feldspar samples approached saturation. Hence, the regeneration method was considered as the best choice.

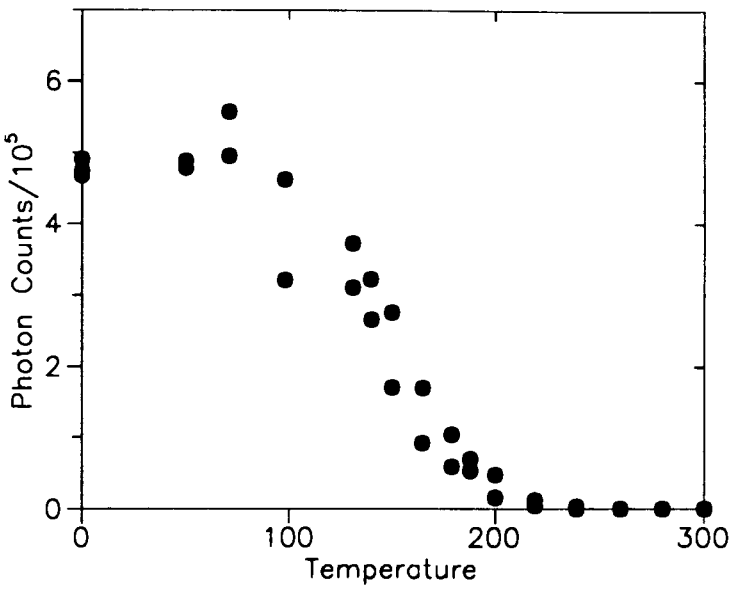

Figure B.3: Luminescence intensity *vs.* preheat temperature for DY23. Two feldspar sample planchets were prepared for each preheat temperature.

In order to determine a preheat temperature, a set of feldspar samples were preheated at various temperatures for an hour and the resulting luminescence was measured. The results are illustrated in figure B.3. From these data, the preheat temperature was chosen to be 150 ℃ for this sample.

Some of the sample planchets were bleached by direct outdoor sunlight exposure for 3 hours. Luminescence was measured after bleaching and the photon count rate from these samples was found to be almost the same as the dark count rate of the apparatus used for the measurement. All natural and bleached sample planchets were then irradiated at various doses and preheated at 150 ℃ for 5 days instead of 1 hour. The preheat time was chosen on the basis of the results obtained by Ollerhead *et al.* (1994) and Huntley *et al.* (1993).

Luminescence was measured from natural (N), γ irradiated (N+γ), and bleached (N+sun, N+sun+γ) sample planchets using the automated 50-sample apparatus. The luminescence data were then summed over 5 s intervals as it was done for peat samples. The maximum likelihood fitting of data and equivalent dose calculation was done using a regeneration program written by D.J. Huntley. The results are shown in figure B.4

and in figure B.5.

The equivalent dose for the feldspar extracts was found to be 1055 ± 100 Gy, which was calculated as the average of the equivalent doses obtained for all the 5 s time intervals.

This sample was also analyzed in order to find the dose rate. The analyzed U, Th, and K contents for this sample are $0.77 \pm 0.06 \mu g/g$, $3.0 \pm 0.1 \mu g/g$, and 2.62%, respectively. The Rb content was found to be $97 \pm 5 \mu g/g$. The K content in the feldspar extracts, on the other hand, was found to be 9.05%. The *in situ* water contents was measured to be 4.59%.

The dose contribution from α particles is negligible in this case because the range of α particle in minerals (25 μm) is quite small compared to the size of the grains selected for dating (180—250 μm). Another reason to ignore the α dose rate is that the outer layer of the feldspar grains was actually removed at the time of sample preparation. Considering the size of the grains and the range of the β and γ particles, the total dose rate for the sample comes from two sources: β and γ dose from the environment and the β dose from within the grains.

The internal β dose rate comes from both K and Rb. It was discovered that the K-feldspar grains which contain the highest potassium content contribute most to the measured luminescence (Spooner 1992, Prescott and Fox 1993). The K content of the grains dominating the luminescence would therefore be higher than the measured value for the feldspar extracts (9.05%). On the other hand, pure K-feldspar contains 14% potassium. The K content was thus taken to be $12 \pm 1\%$ to cover any possibility at 2 standard deviations. The grain size was taken to be 200 ± 20 μm. Because the average range of the β particles is larger than the size of the grains, it is expected that only $7.0 \pm 0.7\%$ of β dose rate would be absorbed by the grains of such a size (Mejdahl 1979).

The dose rate from Rb is 4.68 Gy/ka for each 1% Rb. Also, the β dose from Rb would be completely absorbed by the grains of size 0.1 mm (Mejdahl 1983). There are two ways to estimate the Rb content inside the luminescence-emitting feldspar grains: 1) the ratio of K and Rb contents in pure K-feldspars is usually about 200, this leads to a Rb content to be about 600 μg/g; 2) if we take the ratio of K and Rb contents as

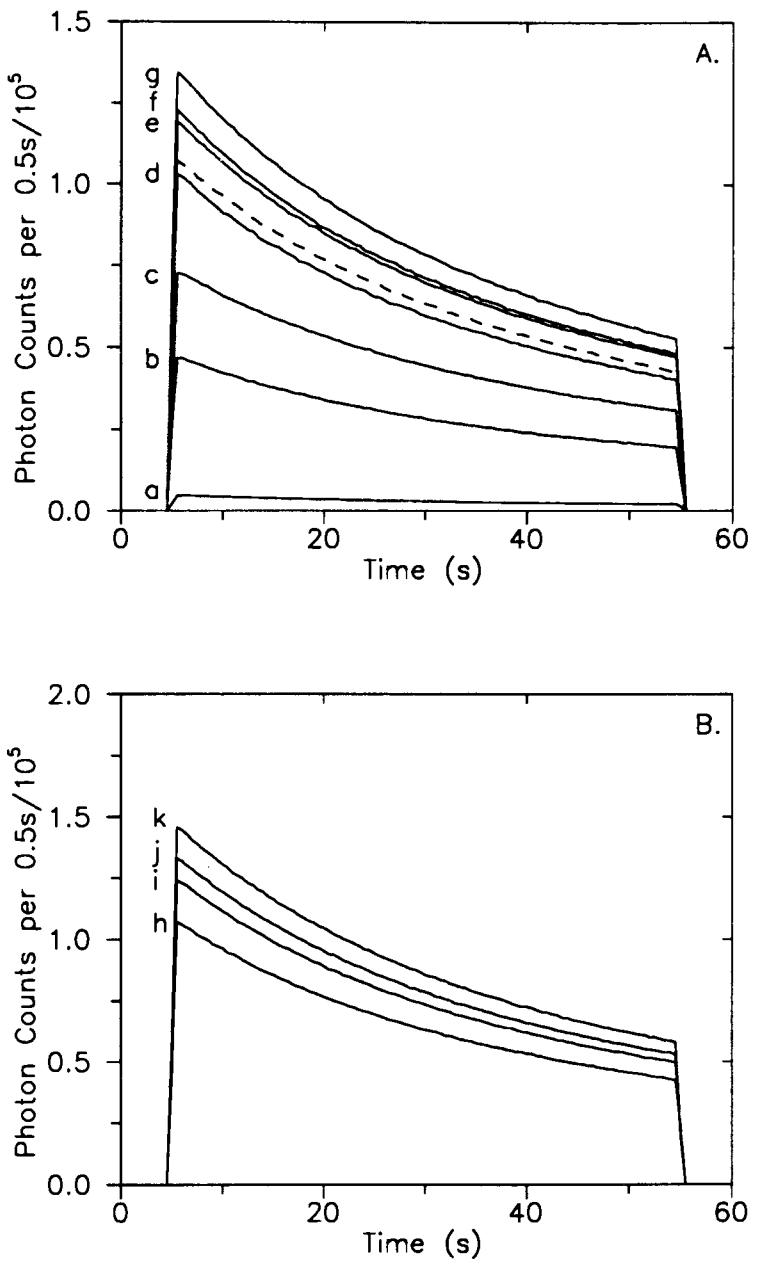

Figure B.4: Data for DY23 feldspar extracts. A. Luminescence decay curves for regenerated samples (n+sun+γ). Each curve shown is the average of measured data for 2 or 3 sample planchets. Solid curves: a. natural+sun; b. 304 Gy; c. 605 Gy; d. 907 Gy; e. 1210 Gy; f. 1512 Gy; g. 1814 Gy. Dashed curve: natural.
B. Luminescence decay curves for N+γ samples. h. natural; i. 304 Gy; j. 605 Gy; k. 907 Gy.

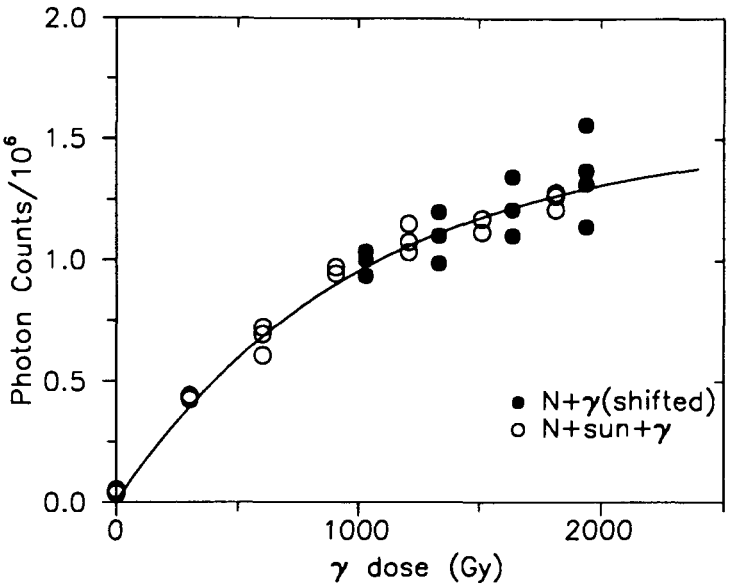

Figure B.5: Additive dose data for DY23 feldspar extracts. Shown is a saturating exponential fit to the regenerated and N+γ data jointly for the first 5 s time interval. The equivalent dose was found to be 1055 ± 100 Gy.

a constant for the whole the sample, the Rb content is then 440 μg/g (the internal K content was taken as 12% as mentioned above). If we assume that the Rb content is within the range 440—600 μg/g and take this range as 2 standard deviation, we can get the Rb content to be 520 ± 40 ppm. The total internal β dose rate from K and Rb was calculated to be 0.93 ± 0.08 Gy/ka using these estimates.

The environmental β and γ dose rates were calculated using the dose rate equations in chapter 5. Since the water content was unlikely to be less than 10% and may have been saturated most of the time in the past (the saturated water content for sands is about 30%), the water content used was taken to be 20 ± 5%. The total external β and γ dose rates were estimated to be 1.86 ± 0.13 Gy/ka and 0.72 ± 0.06 Gy/ka.

From above, the total dose rate for the sample was found to be 3.5 ± 0.2 Gy/ka (excluding the contribution from cosmic rays). Since the contribution from cosmic rays (< 0.2 Gy/ka) is very small compared to the dose rate from within the grains and from the environment, It is apparent that the age for the sample is approximately 300 ka. On the other hand, the total contribution from cosmic rays can be estimated

by considering the extremes of the possible deposition histories: 1) if the sample stayed near the surface all the time (dose rate ~0.2 Gy/ka), the total dose would be about 60 Gy; 2) if the sample has been located at the current position for past 300 ka (dose rate 0.04 Gy/ka), the total dose would be about 12 Gy. The total cosmic dose is therefore lies between 12 and 60 Gy. Assuming that this range covers 2 standard deviation, the total contribution from cosmic rays is thus 36 ± 12 Gy.

The age for the sample is estimated to be 290 ± 30 ka if the cosmic-ray dose is included. Because it is not known whether or not there existed thermal fading or anomalous fading, this age should be regarded as a lower limit of level 3 sand provided that the sample was exposed to sufficient sunlight at the time of deposition. More investigation should be made before an age can be given for the sample.

B.4 Quartz extracts

An attempt was made to obtain the equivalent dose for the feldspar inclusions within quartz as suggested by Huntley *et al.* (1993). A single-sample apparatus was used to achieve a better light collection efficiency because the sample did not give much luminescence (about several hundred counts per second). Although it was found that the luminescence from irradiated samples was higher than that of the bleached samples, there seemed to be no apparent dependence of luminescence on radiation dose as in the case of the feldspar extracts (figure B.6). The normalization factors for the sample planchets also varied drastically from about 0.2 to about 2. It appears that dating of inclusions may not be applicable to this sample. The size of the scatter in the data is quite large even after normalization. The scatter may be a result of anomalous fading and is still not understood.

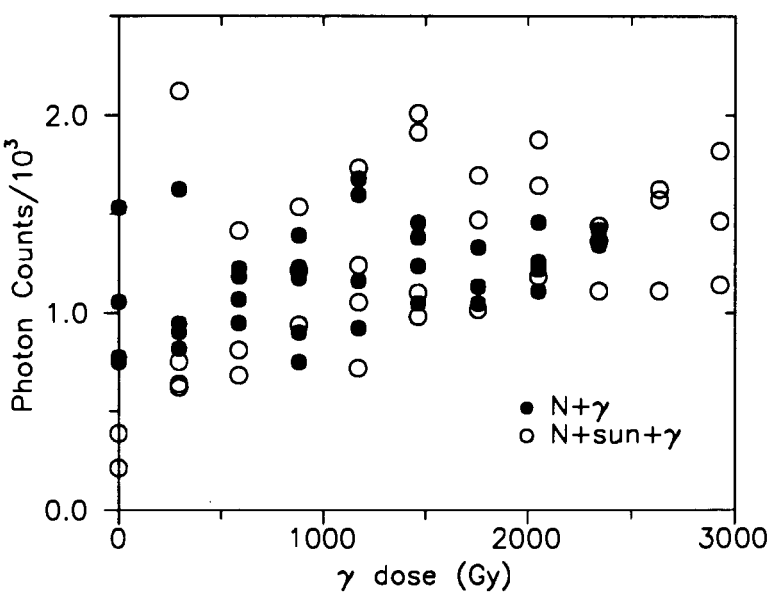

Figure B.6: Additive dose data for DY23 quartz extracts. Shown are the regenerated and N+γ data for the first 5 s time interval. There seems to be little or no apparent dependence of luminescence intensity on radiation dose.

Bibliography

Aitken, M.J. 1985, Thermoluminescence dating, Academic Press, 1985, London.

Aitken, M.J. and Bowman, S.G.E. 1975, Thermoluminescent dating: assessment of alpha particle contribution, *Archeometry*, **17**, 132—138.

Aitken, M.J. and Xie, J. 1990, Moisture correction for annual gamma dose, *Ancient TL*, **8**, 6—9.

Aitken, M.J. and Xie, J. 1992, Optical dating using infrared diodes: young samples, *Quat. Sci. Rev.*, **11**, 147—152.

Alley, N.F. and Hicock, S.R. 1986, The stratigraphy, palynology, and climatic significance of pre-middle Wisconsin Pleistocene sediments, southern Vancouver Island, British Columbia. *Canadian Journal of Earth Sciences*, **23**, 369—382.

Armstrong, J.E. 1990, Vancouver geology. Geological Association of Canada, Vancouver.

Armstrong, J.E. and Clague, J.J 1977, Two major Wisconsin lithostratigraphic units in southwestern British Columbia, *Canadian Journal of Earth Sciences*, **14**, 1471—1480.

Bailiff, I.K. 1993, Measurement of the stimulation spectrum (1.2—1.7 eV) for a specimen of potassium feldspar using a tunable solid state laser,

Bailiff, I.K. and Poolton, N.R.J. 1991, Studies of charge transfer mechanisms in feldspars, *Nucl. Tracks Radiat. Meas.*, **18**, 111—118.

Barbouti, A.I. and Rastin, B.C. 1983, A study of the absolute intensity of muons at sea level and under various thickness of absorbers, *J. Phys. G (GB)*, **9**, 1577-1595.

Bard, E., Hamelin, B., Fairbanks, R.G., and Zindler, A. 1990, Calibration of the C-14 time scale over the past 30,000 years using mass spectrometric U-Th ages from Barbados corals, *Nature*, **345**, 405—410.

Berger, G.W. 1988 , Dating quaternary events by luminescence, in *Dating Quaternary sediments*, edited by D.J. Easterbrook. Geological society of America paper 227, pp. 13—50.

Blunt, D.J., Easterbrook,D.J., and Rutter, N.A. 1987, Chronology of Pleistocene sediments in the Puget Lowland, Washington. *Washington Division of Geology and Earth Resources Bulletin*, **77**, 321—353.

Chen, R. and Kirsh, Y. 1981, Analysis of thermally stimulated processes, Pergamon Press, Oxford.

Deer, W.A., Howie, R.A., Zussman, J. 1966, An introduction to the rock-forming minerals, Longman Group Limited, London.

Ditlefsen, C. and Huntley, D.J. 1994, Optical excitation of trapped charges in quartz, potassium feldspars and mixed silicates: the dependence on photon energy, *Radiat. Meas.*, in press.

Divigalpitiya, W.M.R. 1982, Thermoluminescence Dating of Sediments, M.Sc. thesis, Simon Fraser University.

Duller, G.A.T. and Wintle, A.G. 1991, On infrared stimulated luminescence at elevated temperatures, *Nucl. Tracks Radiat. Meas.*, **18**, 379—384.

Easterbrook, D.J. 1986, Stratigraphy and chronology of Quaternary deposits of the Puget Lowland and Olympic Mountains of Washington and the Cascade Mountains of Washington and Oregon. In *Quaternary glaciations in the northern*

hemisphere. Edited by V. Šibrava, D.Q. Bowen, and G.M. Richmand. *Quaternary Science Reviews*, **5**, 145—159.

Easterbrook, D.J., 1992, Advance and retreat of Cordilleran ice sheets in Washington, U.S.A. *Géographie Physique et Quaternaire,* **46**, 51—68.

Easterbrook, D.J., Crandell, D.R., and Leopold, E.B. 1967, Pre-Olympia stratigraphy and chronology in the central Puget Lowland, Washington. *Geological Society of America Bulletin,* **78**, 13—20.

Easterbrook, D.J., Briggs, N.D., Westgate, J.A., and Gorton, M.P. 1981, Age of the Salmon Springs glaciation in Washington, *Geology*, **9**, 87—93.

Easterbrook, D.J., Roland, J.R., Carson, R.J. and Naeser, N.D. 1988, Application of paleomagnetism, fission-track dating, and tephra correlation to Lower Pleistocene sediments in the Puget Lowland. *Geological Society of America Special Paper 227*, pp. 139—165.

Godfrey-Smith, D.I. 1991, Optical Dating Studies of Sediment Extracts, Ph.D thesis, Simon Fraser University.

Godfrey-Smith, D.I., Huntley, D.J. and Chen, W.-H. 1988, Optical dating studies of quartz and feldspar sediment extracts, *Quat. Sci. Rev.*, **7**, 373—380.

Heusser, C.J., and Heusser, L.E. 1981, Palynology and paleotemperature analysis of the Whidbey Formation, Puget Lowland, Washington. *Canadian Journal of Earth Sciences*, **18**, 136—149.

Hicock, S.R. 1990, Last interglacial Muir Point Formation, Vancouver Island, British Columbia, *Géographie Physique et Quaternaire,* **44**, 337—340.

Hicock, S.R. and Armstrong, J.E. 1983, Four Pleistocene formations in southwest British Columbia: their implications for patterns of sedimentation of possible Sangamonian to early Wisconsinan age. *Canadian Journal of Earth Sciences*, **20**, 1232—1247.

Huntley, D.J., Berger, G.W., Divigalpitiya, W.M.R. and Brown, T.A. 1983, Thermoluminescence dating of sediments. *PACT*, **9**, 607—618.

Huntley, D.J., Godfrey-Smith, D.I., Thewalt, M.L.W. 1985, Optical dating of sediments, *Nature*, **313**, 105—136.

Huntley, D.J., Nissen, M.K., Thomson, J., and Calvert, S.E. 1986, An improved alpha scintillation counting method for determination of Th, U, Ra-226, Th-230 excess, and Pa-231 excess in marine sediments, *Can. J. Earth Sci.*, **23**, 959—966.

Huntley, D.J., Godfrey-Smith, D.I., Thewalt, M.L.W, and Berger, G.W. 1988, Thermoluminescence spectra of some mineral samples relevant to thermoluminescence dating. *Journal of Luminescence*, **39**, 123—136.

Huntley, D.J., Godfrey-Smith, D.I. and Haskell, E.H. 1991, Light-induced emission spectra from some quartz and feldspars, *Nucl. Tracks Radiat. Meas.*, **18**, 127—131.

Huntley, D.J., Hutton, J.T., and Prescott, J.R. 1993, Optical dating using inclusions within quartz grains, *Geology*, **21**, 1087—1090.

Hütt, G., Jaek, I. and Tchonka, J. 1988, Optical dating: K-feldspars optical response stimulation spectra, *Quat. Sci. Rev.* **7**, 381—385.

Hütt, G., Jaek, I. 1989, Infrared stimulated photoluminescence dating of sediments, *Ancient TL*, **7**, 48—51.

Hütt, G. and Jungner, H. 1992, Optical and TL dating on glaciofluvial sediments, *Quat. Sci. Rev.*, **11**, 161—163.

Hütt, G., Jungner, H. and Kujansuu, R. 1993, OSL and TL dating of buried podsols and overlying sands in Ostrobothnia, western Finland, *Journal of Quarternary Science*, **8**, 125—132.

Jungner, H. and Huntley, D.J. 1991, Emission spectra of some potassium feldspars under 633 nm stimulation, *Nucl. Tracks Radiat. Meas*, **18**, 125—126.

Li, S.H. and Wintle, A.G. 1992, A global view of the stability of luminescence signal from loess, *Quat. Sci. Rev.*,**11**, 133—137.

Lian, O.B. 1991, The late quaternary surficial geology and geomorphology of the lower Seymour Valley, North Vancouver, British Columbia, M. Sc. Thesis, Simon Fraser University.

Lian, O.B., and Hickin, E.J. 1991, Late Pleistoncene stratigraphy and chronology of lower Seymour Valley, southwestern British Columbia, *Can. J. of Earth Sci.*, **30**, 841—850.

Marfunin, A.S. 1979, A.S., Spectroscopy, luminescence and radiation centres in minerals, Springer-Verlag, New York, 1979.

McKeever, S.W.S. 1985, Thermoluminescence of solids, London, Cambridge University Press.

Mejdahl, V. 1983, Internal radioactivity in quartz and feldspar grains, *Ancient TL*, **5**, No. 2, 10—17.

Mejdahl, V. 1979, Thermoluminescence dating: beta-dose attenuation in quartz grains, *Archaeometry*, **21**, part 1, 61—72.

Mochanov, Y.A. 1988, The most ancient Paleolithic of the Diring and the problem of a nontropical origin for humanity. Translation in *Arctic Anthropology*, **30**, 22—53, 1993.

Nambi, K.S.V. and Aitken, M.J. 1986 , Annual-dose conversion factors for TL and ESR dating, *Archaeometry*, **28**, 263—269.

Ollerhead, J., Huntley, D.J. and Berger, G.W. 1994, Luminescence dating of sediments from Buctouche Spit, New Brunswick, *Can. J. Earth Sci.* 1994, **31**, 523—531.

Prescott, J.R. and Fox, P.J. 1993, Three dimensional thermoluminescence spectra of feldspars, *J. of Phys. D, Applied Physics*, **26**, 2245-54.

Prescott, J.R. and Hutton, J.T. 1994, Cosmic-ray contribution to dose rate for luminescence and ESR dating: large depths and long-term time variations, *Radiat. Meas.*, in press.

Ryder, J.M. and Clague J.J. 1989, *British Columbia (Quaternary stratigraphy and history, Cordilleran Ice Sheet)*, In *Quaternary geology of Canada and Greenland*, edited by R.J. Fulton. Geological survey of Canada, Geology of Canada, No.1, 45—58 (Also Geological Society of America, The Geology of North America, vol. K-1).

Short, M.A. 1993, Some aspects of optically stimulated luminescence for sediment dating, M. Phil. Thesis, University of Hong Kong.

Spooner, N.A. 1992, Optical dating: preliminary results in the anomalous fading of luminescence from feldspar, *Quat. Sci. Rev.*, **11**, 139—145.

Spooner, N.A. 1993, The validity of optical dating based on feldspar, PhD thesis, Oxford University.

Van der Wijk, A., El-Daoushy, F., Arends, A.R., and Wook, W.G. 1986, Dating peat with U/Th disequilibrium: some geochemical considerations. *Chemical Geology*, **59**, 283—292.

Westgate, J.A., Easterbrook, D.J., and Carson, R.J. 1987, Lake Tapps tephra: an early Pleistocene stratigraphic marker in the Puget Lowland, Washington. *Quaternary Research*, **28**, 340—355.